Frequent activity on Vulcano (Italy) spanning the last 80 ky: new insights from the chemo-stratigraphy of the Brown Tuffs

S. Meschiari [(a)], P.G. Albert [(b, c)], F. Lucchi [(a)], R. Sulpizio [(d)], V.C. Smith [(c)], R. Kearney [(c)], C.A. Tranne [(a)].

(a) Dipartimento di Scienze Biologiche, Geologiche e Ambientali, Università di Bologna, Piazza Porta S. Donato 1, 40126 Bologna, Italy

(b) Department of Geography, Swansea University, Singleton Park, Swansea SA2 8PP, UK

(c) Research Laboratory for Archaeology and the History of Art (RLAHA), University of Oxford, Dyson Perrins Building, South Parks Road, Oxford OX1 3QY, UK

(d) Dipartmento di Scienze della Terra e Geoambientali, Universitá di Bari, via Orabona 4, 70125 Bari, Italy

E-mail address: sara.meschiari4@unibo.it (S. Meschiari).

ABSTRACT

The Brown Tuffs (BT) are widespread reddish-brown to grey, ash-rich pyroclastic deposits recognized in the stratigraphic sequences of the Aeolian Islands and Capo Millazzo peninsula (Sicily) that span the last 80 ky. They have very homogeneous lithological, textural and sedimentological features which make it difficult to reliably correlate units on the islands to proximal units in the source areas. Here we carefully re-interpret the stratigraphic profiles of the BT on Vulcano and Lipari where the deposits are thickest and present the most complete succession. The investigation is based on a large dataset of major and minor element geochemistry of juvenile glass components for the majority of the recognized BT depositional units, whilst also providing new radiocarbon ages. The distinctive chemical groupings observed within the glass analyses, both temporally and spatially, allow us to fingerprint the three main stratigraphically defined macro-units in which the BT succession can be sub-divided using prominent tephra marker beds, the Ischia Tephra (Monte Epomeo Green Tuff; 56 ky) and Monte Guardia pyroclastics from Lipari (herein radiocarbon dated to 27-26 ky). The Lower (80-56 ky; LBT), Intermediate (56-27 ky; IBT) and Upper BT (here dated at 24-6 ky; UBT) macro-units display K-series volcanic glasses ranging from basaltic trachy-andesites, through trachy-andesites, to more evolved trachytes, all consistent with an origin on Vulcano. The UBT are clearly distinguished from the lower macro units by their higher-SiO_2 trachy-andesite to trachytic glasses, which extend to noticeably lower TiO_2, CaO and MgO contents. These features make it possible to re-define the geochemical-evolutionary boundary between IBT and UBT as corresponding to the 24 ky Spiaggia Lunga scoria bed on Vulcano, which is stratigraphically higher (and younger) than the previous boundary marker (Monte Guardia). The glass compositions of the LBT, IBT and UBT are used to: (1) assess links to known proximal eruption units outcropping on Vulcano; (2) validate medial-distal BT occurrences across the Aeolian archipelago (Salina, Filicudi and Panarea) and on Capo Millazzo; (3) confirm that the BT are responsible for distal volcanic ash layers preserved in Central Mediterranean marine sedimentary archives. Interestingly, the glass compositions of the UBT are very similar to those of the Punte Nere unit, the earliest pyroclastic products erupted from the currently active La Fossa cone on Vulcano, indicating the corresponding magmatic system has likely erupted similar melts and products over the last 24 ky and thus extending its life cycle. Such information is crucial for evaluating the long-term eruption scenarios underpinning hazard assessment of the La Fossa caldera magmatic system.

1. INTRODUCTION

Explosive volcanic eruptions can disperse volcanic ash (< 2 mm) to distances of tens to thousands of kilometers from their source and cause multi-hazard impacts on human activities and the environment, potentially forcing climate variability (e.g. Martin et al., 2009; Le Pennec et al., 2011; Bonasia et al., 2012; Sulpizio et al., 2012; 2014; Biass et al., 2014; Dingwell and Rutgersson, 2014; Scaini et al., 2014). Pyroclastic deposits from these eruptions are crucial for reconstructing the volcanic history of a volcano, and understanding the frequency and the impact of its eruptive activity on the surroundings. Where the age of the corresponding eruptions is known, ash (tephra) deposits preserved in distal sedimentary records are also powerful chronological and stratigraphic markers in complex stratigraphic sequences across the region (Narcisi, 1996; Machida, 1999; Shane, 2000), and can be used in age-depth models and to synchronize disparate sedimentary palaeoclimate archives (Paterne et al., 1986; 1988; Sulpizio et al., 2010; Zanchetta et al., 2011).

In this paper, the Brown Tuffs (BT) are presented as a case study of widespread, ash-rich pyroclastic deposits. These deposits have metric thickness and are recognized in the stratigraphic sequences of most of the Aeolian Islands and on the Capo Milazzo peninsula in northern Sicily. Their interpretation as paleosols, reworked or primary pyroclastic products, as well as their vent locations, areal distribution, chronology and eruptive processes has been long debated (Bergeat, 1899; Pichler, 1980; Keller, 1967; Keller, 1980a, b; Crisci et al., 1981, 1983, 1991; Manetti et al., 1988, 1995; Morche, 1988; Gioncada et al., 2003). Stratigraphic and tephrochronological studies have suggested that the BT are composed of a number of depositional units emplaced in the 80-5 ky time interval by pyroclastic density currents (PDCs) and fallout from hydromagmatic explosive activity of a vent (or multiple vents) located within the La Fossa caldera on Vulcano (Lucchi et al., 2008; 2013b). This is also confirmed by measurements of the anisotropy of magnetic susceptibility of BT sequences on Lipari and Vulcano (Cicchino et al., 2011) and combined textural, petrological methods on glass fragments of the BT on Lipari (De Rosa et al. 2016). However, in most outcrops the BT show a very homogeneous lithology, whilst sedimentological characteristics and textural features, reflecting similar eruptive mechanisms, transport and deposition. Moreover, preliminary glass compositional data indicate the deposits have a dominant, albeit variable, trachy-andesite glass composition and overall K-series affinity, extending towards subsidiary rhyolitic components (Lucchi et al., 2008). As a consequence, the individual BT depositional units generally cannot be distinguished from each other, and only separated by localized erosive surfaces or reworked horizons and the interbedding of other volcanic units or exotic tephra deposits erupted from within, and outside the Aeolian Islands. A stratigraphic subdivision into three macro-units, namely the Lower (LBT), Intermediate (IBT) and Upper BT (UBT), has been proposed by Lucchi et al. (2008, 2013b) based on the interbedding of two stratigraphic markers correlated on a regional scale, namely the i) Ischia Tephra (56 ky) from Campania and the ii) Monte Guardia pyroclastics (27-24 ky) from Lipari. Unfortunately, the discontinuous recognition of these marker-beds makes difficult to correlate directly the BT macro-units between one island and another, and throughout the Aeolian archipelago. The similar componentry and mineral assemblage, and the rather small glass compositional variability reported so far (Lucchi et al. 2008, 2013b; De Rosa et al., 2016), has meant that the LBT, IBT and UBT could not be clearly discriminated or correlated across the islands in the absence of the interlayered marker-beds. Because of all these difficulties and fragmentary stratigraphic, petrological and geochemical data, a largely accepted framework of the distribution and depositional area of these units and their correlation to proximal counterparts on the island of Vulcano (for the LBT and IBT) has been missing.

Here we present a large dataset of major and minor element geochemistry of juvenile glass components for most BT depositional units using grain-specific micro-analytical techniques. The BT were sampled from exposed stratigraphic profiles on the islands of Vulcano and Lipari, which are fully representative of the complete stratigraphic succession, together with selected stratigraphic sections from the islands of Salina, Filicudi, Panarea and on Capo Milazzo peninsula (northern Sicily) for strengthening the correlations. A revised stratigraphic analysis of the BT exposures has taken advantage of the local successions, new radiocarbon ages and correlation of marker beds to the regional tephrostratigraphy (e.g. Albert et al., 2017). This provides an improved reconstruction of the stratigraphy, dispersal and chronology of the different BT depositional units. The LBT, IBT and UBT macro-units are geochemically fingerprinted in order to investigate the compositional variability both temporally and spatially, supporting inter-island and regional correlations. Previously the BT were largely overlooked as correlatives of volcanic ash recorded in distal land and deep-sea archives (Paterne et al., 1986, 1988; Siani et al., 2004; Di Roberto et al., 2008; Albert et al., 2012; Caron et al., 2012; Insinga et al., 2014; Matthews et al., 2015; Tamburrino et al., 2016), mostly due to an inadequate characterization of their glass geochemistry. This contribution instead illustrates that the BT are potentially proximal (high-volume) equivalents of widespread ash dispersals, with the associated tephra layers being suitable to correlate volcanic and tectonic events across the whole Aeolian archipelago and southern Tyrrhenian

Sea. Finally, the glass geochemical data of the LBT, IBT and UBT, combined with stratigraphic and lithological information, are also used to infer links to proximal units on Vulcano, providing insights into the eruptive and magmatic history and long-term hazard assessment in the La Fossa caldera magmatic system.

2. STUDY AREA

The Aeolian Islands (Alicudi, Filicudi, Salina, Lipari, Vulcano, Panarea and Stromboli; Fig. 1a), and the surrounding seamounts, are an active volcanic system in the southern Tyrrhenian Sea (Barberi et al., 1973, Beccaluva et al., 1985; De Astis et al., 2003; Chiarabba et al., 2008; Ventura, 2013). Subaerial volcanism developed from c. 270–240 ky to the present (Leocat, 2011; Lucchi et al., 2013b), through successive eruptive epochs subdivided by volcanic collapses or major quiescent (erosional) stages (De Astis et al., 2013; Forni et al., 2013; Francalanci et al., 2013; Lucchi et al., 2013 a,c,d,e), and the erupted melts range from basaltic andesites to rhyolites, covering a large spectrum of differing magmatic suites from calc-alkaline (CA), high-K calc-alkaline (HKCA), shoshonitic (SHO) and K-Series (KS) (Ellam et al., 1988; Francalanci et al., 1993; Peccerillo et al., 2013). Vulcano, which is the suggested source area of the Brown Tuffs (BT), is a complex volcanic system made up of various eruptive centres and two multi-stage calderas (Il Piano and La Fossa), and characterized by the active La Fossa cone (De Astis et al. 2013). The BT have been deposited during distinct time intervals over the last c. 80 ky (Lucchi et al., 2008, 2013b), and are interlayered with widespread fall deposits from major explosive eruptions of Lipari, Stromboli, Salina and Campania (Keller, 1981; Lucchi et al., 2013b; Albert et al., 2017).

3. METHODS

3.1. Fieldwork

Stratigraphic analysis and sampling was conducted principally on the islands of Vulcano and Lipari, whilst also on Salina, Panarea, Filicudi and Capo Milazzo peninsula following the correlations between islands as defined by Lucchi et al. (2008, 2013b). Stratigraphic logging and lithostratigraphy focussed on identifying all the individual depositional units of the BT, and obtain a comprehensive set of samples of the tephra deposits. Following Lucchi (2013), a “depositional unit” is generically referred to as the pyroclastic material deposited during an individual, relatively continuous eruptive event (PDC or fallout), and is delimited by features indicative of interruptions of deposition or energy variations (e.g. erosive surfaces, paleosols, reworked horizons, angular discordances, sharp grain-size variations, fine ash layers), or other volcanic units.

Once the stratigraphic correlations of the BT across the islands had been fixed, 65 ash deposits were sampled covering most of the BT depositional units that were stratigraphically recognized, together with several lapilli (12) and ash (19) samples from the interbedded tephra layers. We also sampled near-vent pyroclastic deposits on Vulcano which either represent potential proximal equivalents of the BT (Monte Molineddo 1-3 and Punte Nere formations; De Astis et al., 2013), and/or offer useful constraints on the known chemical signature of the volcano.

3.2. Laboratory analyses

Juvenile (glass) fragments from the selected samples were washed, dried and mounted in Streurs epoxy resin. Mounts were ground, polished and carbon coated in preparation for chemical analysis. Major and minor element micron-beam volcanic glass data was determined using the wavelength-dispersive JEOL 8600 and the JEOL 8200 electron microprobes (WDS-EMP) at the Research Laboratory for Archaeology and the History of Art (RLAHA), University of Oxford. Details of the analytical operating conditions, monitoring of data accuracy and precision, and post-analysis data treatment are provided in Supplementary Material A.1. The full geochemical dataset, along with MPI-DING reference glasses (Jochum et al., 2006) run alongside the unknown samples are available in Supplementary Material B. Data presented in plots are normalised (e.g., water-free) and error bars represent reproducibility, calculated as 2 x standard deviation of replicate analysis of StHs6/80-G reference glass.

Charcoal fragments embedded within the BT deposits were collected for radiocarbon (^{14}C) dating to provide further age constraints. Charcoals were chemically pre-treated at the Oxford Radiocarbon Accelerator Unit (ORAU) using the acid- base-acid (ABA) methodology outlined by Brock et al. (2010). The ^{14}C analyses were subsequently performed using a 2.5 MV HVEE tandem Accelerator Mass Spectrometry (AMS) system at ORAU (Ramsey et al., 2004). These new radiocarbon ages, together with previously published BT radiocarbon ages (Pichler, 1980; Crisci et al., 1981, 1983; De Astis et al., 1997), were then calibrated and modelled using the Bayesian statistical program of OxCal v4.4 (Bronk Ramsey, 2009), using the IntCal20 Northern Hemisphere calibration curve (Reimer et al., 2020).

4. RESULTS

4.1. Overview of the stratigraphy and age of the Brown Tuffs (BT)

The BT are made up of reddish-brown to grey fine to coarse ash in weakly coherent to coherent depositional units, which comprise glass shards, minor crystals (with abundant clinopyroxene) and a negligible lithic content. They form thick massive successions (up to 15-25 m on Vulcano and Lipari) with considerable thickness variations due to the paleo-topography and erosion. In some exposures on Vulcano and southern Lipari there are internal grain size variations, color banding and plane-parallel to cross bedding stratification (De Astis et al, 1997; Lucchi et al., 2008). The stratigraphy of the BT has been reviewed through a careful investigation of the majority of the outcrops on the islands of Vulcano and Lipari (Fig. 1), where the BT obtain their maximum thickness, and where there are radiocarbon (^{14}C) age constraints. Outcrops on Salina, Filicudi, Panarea and Capo Milazzo (Fig. 1) were also studied to verify BT occurrences and extend the correlations established on Vulcano and Lipari. The outcrops of the BT on Capo Milazzo, originally described by Morche (1988), are now largely eroded and partially destroyed by anthropogenic activity. The BT outcropping on the islands of Alicudi and Stromboli are not considered here due to their poor stratigraphic and chronologic constraints (Francalanci et al., 2013; Lucchi et al., 2013d). The most important features of the Campanian and Aeolian tephra layers ultimately used to subdivide and correlate the BT are provided in Table 1, and the suite of radiocarbon ages adopted in the present work is provided in Table 2.

The most complete succession of the BT is reconstructed on the island of Lipari, furtherly detailing the stratigraphy previously proposed by Lucchi et al. (2008, 2013b) by identifying a few more interlayered tephra beds and localized erosional surfaces. The BT succession is distinguished into (at least) 16 depositional units (Fig. 2), superimposed on the three-fold subdivision into the Lower (LBT), Intermediate (IBT) and Upper BT (UBT) macro-units based on the interbedded Ischia Tephra and Monte Guardia pyroclastics from Lipari (see Lucchi et al., 2013b and references therein). The most important features of this succession are hereafter described, outlining correlations between the main outcrops on Lipari and Vulcano, and the other Aeolian Islands and the Capo Milazzo peninsula. Correlations with the island of Vulcano are described below in Section 4.1.1.

The LBT are constrained at the base by the late marine (oxygen) isotope stage (MIS) 5 conglomerate deposits (c. 80 ky) along the west coast of Lipari, as well as on Salina, Filicudi, Panarea and the Capo Milazzo peninsula. A lower chronological boundary is also provided by lapilli and ash correlated to the 77-75 ky Petrazza Tuffs from Stromboli found at the base of the LBT succession on Panarea and Capo Milazzo (Lucchi et al. 2008 and references therein). The Grey Porri Tuffs (GPT) from Salina (70-67 ky; Sulpizio et al., 2016 and references therein) are important for stratigraphic correlations in the lower portion of the LBT on Salina and Lipari, with distal occurrences on Panarea and Capo Milazzo.

The IBT are defined as above the Ischia Tephra, which is widely exposed on Lipari, Salina, Filicudi and Panarea. This marker bed is the distal equivalent of the Monte Epomeo Green Tuff of Ischia (Tomlinson et al., 2014), and dated distally in Lake Fucino (Italy) at 56.1 ± 1.0 ky [2σ] (Giaccio et al., 2017). The IBT are best exposed in southern-central Lipari (Fig. 3A-B) where they are split into (at least) 6 depositional units by the local pumiceous successions of Punta di Perciato (undated) and Falcone (43-40 ky; Forni et al 2013 and references therein), the Lower Pollara Tuffs from Salina and a couple of other tephra layers (Fig. 2, Table 1). Particularly, the Lip1 tephra has a rhyolitic composition (cf. 4.2.2.1) and provides evidence of a previously unknown explosive eruption in the southern dome-field of Lipari.

The IBT and UBT macro-units are subdivided on Lipari (Fig. 3A-D) and across much of the archipelago by the Monte Guardia marker bed (Lucchi et al., 2008), until now dated to between 27 and 24 ky (Lucchi et al. 2013b; Albert et al., 2017 and references therein). Here we provide new radiocarbon ages of charcoal remnants embedded within the BT above the Monte Guardia (Table 2), yielding calibrated (IntCal20) eruption ages of 25,845-26,310 cal y BP (95.4%; sample LIP07/17) and 23,830-24,240 cal y BP (95.4%; sample LIP14/17) for the host BT depositional unit. Here we incorporate these new ages, together with all the available and stratigraphically relevant BT ^{14}C ages from the literature (Table 2), into the Bayesian age-model developed by Albert et al. (2017) (Supplementary Material A.3) to provide a more precise age of between 25,920-27,025 cal y BP (95.4%) for the Monte Guardia eruption. The modelling also provides an age of 26,425-27,585 cal y BP (95.4%) for the Lower Pollara eruption (Salina).

The youngest UBT units, above the Monte Guardia marker-bed, are best exposed in the north-eastern sector of Lipari, where they are further subdivided into (at least) 4 distinct depositional units by local pyroclastic deposits (Fig. 2). Most of the UBT are found stratigraphically below the Vallone Canneto Dentro pyroclastic unit (currently undated) (Fig. 3D), with no occurrences between Vallone Canneto Dentro and the widespread Vallone del Gabellotto pyroclastic marker bed (8,430–8,730 cal y BP; Siani et al., 2004; Albert et al., 2017). The most recent UBT depositional unit is recognized between Vallone del Gabellotto and the Monte Pilato pyroclastic unit (dated to 776 CE; Forni et al. 2013, and references therein) (Fig. 3E), and is capped by an irregularly thick reddish paleosol with a maximum age of 5,445-5,610 cal y BP based on previous ^{14}C age determinations (Pichler, 1980; Table 2).

4.1.1. Stratigraphy and age of the BT on Vulcano

The BT deposits are recognized in different sectors of Vulcano, interlayered between various other local volcanic units at different stratigraphic levels (Fig. 2). They do not outcrop in the northern sector of the island (except to the south of M. Lentia) and within the La Fossa caldera owing to their burial by the most recent volcanic products related to the La Fossa and Vulcanello eruptive centres (younger than 5.5 ky).

The youngest UBT are best exposed in the central sector of Il Piano, beyond the south-eastern rim of the La Fossa caldera, and match stratigraphically and lithologically the so-called Piano Grotte dei Rossi tuffs (Lucchi et al., 2008 and references therein). The UBT are subdivided by the widespread Cugni di Molinello scoria fallout layer that is the marker bed (currently undated) separating the lower and upper portions of the Piano Grotte dei Rossi tuffs (‘Tufi di Grotte dei Rossi’ in De Astis et al. 1997). As with the UBT, the source area of the Cugni di Molinello unit is interpreted as being within the La Fossa caldera (De Astis et al., 2013; Dellino et al., 2011). The UBT below Cugni di Molinello contain most of the deposit volume (Fig. 2), with a maximum thickness of 8-10 m along the border of La Fossa caldera, whilst the UBT above the marker bed are only 2-3 m thick and are further subdivided into (at least) 3 depositional units based on the interlayered Monte Saraceno unit (8.3 ky; De Astis et al. 1989) and the Vallone del Gabellotto tephra layer from Lipari (8.7-8.4 ky). Outside of the main depositional area of Il Piano, the UBT are recognized above the Monte Guardia in the areas of Gelso (south-east) and Monte Luccia (central-north Vulcano), and above the Spiaggia Lunga unit (24 ky; Soligo et al. 2000) along the western slopes of the island (Fig. 3F), cropping out very discontinuously due to erosion along steep and exposed slopes. The UBT are not recognized along the western rim of La Fossa caldera, stratigraphically above the intermediate Monte Lentia lava domes (15-13 ky). This suggests that most of the UBT were emplaced before 15-13 ky, likely corresponding to the part of UBT below the Cugni di Molinello marker bed. One of the youngest UBT depositional units has a calibrated radiocarbon age of 8,305-8,655 cal y BP (Table 2). At the top, the UBT are unconformably covered by the Grotta dei Palizzi 1 and 2 pyroclastic successions from the intermediate La Fossa cone (2.9-2.1 ky; De Astis et al., 2013 and references therein) along the border of La

Fossa caldera, whereas there are no clear stratigraphic contacts or field-based correlations with the Punte Nere pyroclastics (Fig. 2) that represent the oldest portion of La Fossa cone succession (5.5-3.8 ky; De Astis et al., 2013 and references therein).

Delimiting the areal distribution of LBT and IBT on Vulcano is challenging, and their separation is made difficult by the absence of the Ischia Tephra marker bed. LBT-IBT deposits with a maximum thickness of 5-6 m are found in south Vulcano near Gelso, below the Monte Guardia marker bed. Whilst, they are generically recognized below the Spiaggia Lunga scoriae in west Vulcano near to Grotta dei Pisani (Fig. 3G), where they show a thickness of 7-8 m, and the absence of the Monte Guardia makes it difficult to define the boundary with the UBT. In this outcrop the LBT-IBT boundary is represented by a high-angle erosional unconformity.

Noteworthy, there are no typical LBT-IBT deposits in the area of il Piano, where the stratotype of UBT is identified. There, three thick pyroclastic successions (Fig. 3H), namely the Monte Molineddo (MM) 1-3 formations (De Astis et al., 2013), are stratigraphically recognized above the Monte Aria/Timpa del Corvo lava flows (78-77 ky; De Astis et al., 2013 and references therein) and below the UBT, matching the stratigraphic position of the LBT-IBT units. Local volcanic units (Monte Rosso, Monte Luccia, Passo del Piano) dated to 53-48 ky (De Astis et al. 2013, and references therein) are interlayered between the MM1-2 and MM3 successions (Fig. 2). The MM1-3 are massive to stratified, grey to varicoloured ash successions with interlayered layers of black to yellow scoria lapilli, which are related to an undefined source area within the La Fossa caldera based on a substantial southeastwards thickness and grain size decrease (De Astis et al., 2013). They share some lithofacies observed in LBT-IBT deposits, but a clear lithostratigraphic correlation has not yet been defined. Remarkably, black to yellow scoria lapilli resembling those of the MM3 succession are found embedded, in places aligned in trails, within the IBT in south Lipari (above the Falcone domes) and near Grotta dei Pisani and Gelso on Vulcano, thus suggesting a possible correlation between the MM3 and IBT.

4.2 Volcanic glass geochemistry of the BT

Following the stratigraphy outline above, in the following sections we report the compositional data (major and minor elements) of volcanic glass (ash and scoria) sampled from throughout the BT successions outcropping on Vulcano and Lipari. Owing to more extensive exposures the chemical analysis of the LBT and IBT stratigraphic macro-units concentrated predominantly on outcrops studied on Lipari, whilst chemical investigations of the UBT instead largely focused on the outcrops exposed on Vulcano (Fig. 4).

For each stratigraphically defined macro-unit outlined below, in the first instance we report the glass data relating to dominant glass component or melt composition tapped during the eruptions responsible for the emplacement of the BT deposits. Overall the juvenile BT glasses range from basaltic trachy-andesites through trachy-andesites to more evolved trachytes (Fig. 5A) and show a clear K-series affinity (Fig. 5B). Major and minor element glass analyses of representative BT depositional units analysed are reported in Table 3 and 4, whilst the full glass dataset is reported in the Supplementary Material B.

Separately, some minor chemical components with distinct compositions are observed within some of the individual BT depositional units (Table 5) and are also described below. We attribute these chemical components to the stratigraphic units underlying the BT, and as such are considered 'secondary' components unrelated to the juvenile products of the BT source eruptions. Specifically, some depositional units in the IBT and UBT contain HKCA rhyolitic glasses, whilst transitional CA to HKCA andesite to dacitic glasses are recognised in some LBT depositional units (Fig. 5A).

To assess links between the BT depositional units and proximal eruptive units on Vulcano we provide additional major and minor element glass data for the Monte Molineddo (MM) 1-3 successions, and the Punte Nere Formation (Table 6). A detailed description of their glass compositions is reported in Supplementary Material A.2.

4.2.1 Glass geochemistry of the LBT outcropping on Lipari and Vulcano

The sampled units representative of the LBT (Bt1-6) outcropping on Lipari are dominated by volcanic glass compositions ranging from basaltic trachy-andesites to trachy-andesites and tephri-phonolites (SiO_2 = 52.4-57.2 wt.%; Na_2O + K_2O = 7.7-11.5 wt.%; [*n* = *109*] Fig. 5A), and these glasses have a clear K-series affinity (K_2O = 4.2-6.3 wt.%; Fig. 5B). Using increasing SiO_2 content as a fractionation index for the LBT glasses, CaO (4.9-7.5 wt.%), MgO (1.8-3.5 wt.%), and Na_2O (2.8-5.9 wt.%) contents noticeably decrease, whilst K_2O content increases. There is no evidence of clear chemo-stratigraphic variation in the glass compositions of the LBT depositional units (Table 3). Trachy-andesite glasses (*n=22*) from the limited LBT exposures accessible on Vulcano, at Grotta dei Pisani, display a consistent K-series affinity, and evolutionary trends similar to those from LBT deposits examined on Lipari (Fig. 5-8).

A secondary glass component (*n=14*), with glasses ranging from andesite through to dacite (SiO_2 = 56.5-62.6 wt.%; Na_2O + K_2O = 4.5-8.3 wt.%) and a transitional CA to HKCA affinity (Fig. 5A), is observed in the LBT units outcropping on Lipari interlayered with (Bt3) and overlying (Bt4) the GPT (Fig. 2).

4.2.2 Glass geochemistry of the IBT outcropping on Lipari and Vulcano

The sampled units representative of the IBT (Bt7-11) that outcrop on Lipari are dominated by volcanic glass compositions ranging from basaltic trachy-andesite to trachy-andesites and tephri-phonolites (SiO_2 = 50.8-57.2 wt.%; Na_2O + K_2O = 7.0-12.3 wt.%; [*n = 279*] Fig. 5A), and these glasses display a clear K-series affinity (K_2O = 3.6-7.5 wt.%; Fig. 5B). Using increasing SiO_2 content as a fractionation index the IBT glasses show decreasing CaO (4.0-9.1wt.%) and MgO (1.3-4.4 wt.%) content, while K_2O increases with evolution (Fig. 5B). The FeOt, TiO_2, Na_2O and Al_2O_3 contents remain broadly constant with increasing SiO_2. No clear chemo-stratigraphic relationship exists in the IBT succession on Lipari (Table 3). The least evolved products observed within the IBT relate to layers of diffuse scoria lapilli (Fig. 7-8; Table 3). The limited IBT exposures on Vulcano at Grotta dei Pisani are relatively homogeneous and chemically consistent with the trachy-andesite/tephri-phonolitic glasses of the IBT on Lipari (Fig. 5A), and these glasses conform to the same evolutionary trends (Fig. 8).

Minor secondary glass components (*n = 34*) observed in distinct IBT depositional units sampled on Lipari (bt8-10) are homogeneous high-SiO_2 rhyolites (SiO_2 = 76.0 ± 0.4 wt.%; Na_2O + K_2O = 8.9 ± 0.3 wt.%; Fig. 5A), and are characterized by variable K_2O contents, but all show a clear HKCA affinity (K_2O = 5.6 ± 0.8 wt.% [2 s.d.]; Fig. 5B). No rhyolitic glasses were observed in the IBT (Bt7) that underly the lowermost Punta di Perciato pumice deposits in southern Lipari (Fig. 2). Separating Bt9 and Bt10 in southern Lipari (Fig. 4; Loc. 3) a previously unreported whitish tephra layer (Lip1, sample LIP01/16; Table 1) was identified, which displays a homogeneous HKCA rhyolitic glass composition (SiO_2 = 75.8 ± 0.6 wt.% [2 s.d.]; K_2O = 5.3 ± 0.4 wt.% [2 s.d.]; *n= 15; Supplementary Material 2*).

4.2.2.1 IBT 'upper' unit that outcrops on Lipari and Vulcano

A further subdivision of the BT succession is introduced here on the basis of the presented volcanic glass chemistry. The glasses analysed from the basal portion of the UBT macro-unit, as previously defined by Lucchi et al. (2008) immediately overlying the Monte Guardia tephra on Lipari and Vulcano (Gelso), and labelled the Bt12 depositional unit here, are actually chemically consistent with the underlying IBT compositions described above (Section 4.2.2; Fig. 6), and distinct from the UBT (Bt13-16). Thus, we prefer to attribute the Bt12 deposits, directly overlying the Monte Guardia, to the IBT macro-unit, and herein name them as the IBT 'upper'.

On Lipari, the IBT 'upper' have a dominant juvenile glass component that ranges from trachy-andesites to higher alkali content tephri-phonolites (SiO_2 = 53.1-55.9 wt.%; Na_2O + K_2O = 8.4-12.3 wt.%; [*n = 157*] Fig. 5A), and these glasses display a clear K-series affinity (K_2O = 5.4-7.5 wt.%; Fig 5B). At Gelso on Vulcano (VUL09/17), the IBT 'upper' is characterised by tephri-phonolitic glasses (Fig. 5A), with a K-series affinity (Fig. 5B), that are consistent with the IBT 'upper' glasses observed on Lipari. With increasing SiO_2 content these IBT 'upper' glasses show broadly increasing K_2O content, decreasing CaO and MgO, whilst FeOt, TiO_2, Na_2O and Al_2O_3 contents remain largely constant. The evolutionary trends of the IBT 'upper' glasses characterised here on both Lipari and Vulcano are entirely consistent with the underlying IBT deposits (Section 4.2.2; Fig. 6).

Minor secondary glass components (*n=19*) observed in the IBT 'upper' on Lipari and Gelso (Vulcano), above the Monte Guardia marker bed, are relatively homogeneous high-SiO_2 rhyolites (SiO_2 = 74.2-77.2 wt.%; Na_2O + K_2O = 8.5-9.9 wt.%; Fig. 5A), these glasses show a clear HKCA affinity (K_2O = 4.8-6.0 wt.%; Fig. 5B).

4.2.3 Glass geochemistry of the UBT

4.2.3.1 UBT units that outcrop on Vulcano, and the Cugni di Molinello Formation

Here we refer to the UBT depositional units (from Bt13 upwards) as those above the IBT 'upper' (Bt12) (Fig. 2). Overall the juvenile glass compositions of the UBT on Vulcano show a considerable range in evolution and are dominated by trachy-andesitic through to trachytic glasses (SiO_2 = 55.7-64.5 wt.%; Na_2O + K_2O = 8.3-11.6 wt.%; *n = 242*; Fig. 5A), all showing a clear K-series affinity (K_2O = 5.1-7.3 wt.%; Fig. 5B). The UBT glass compositions display increasing K_2O and decreasing CaO (2.6-5.7 wt.%), MgO (1.3-2.9 wt.%), and FeOt (3.9-7.3 wt.%) with increasing SiO_2 content, whilst Na_2O (2.6-4.8 wt.%), TiO_2 (0.5-0.8 wt.%; Fig. 5C) and Al_2O_3 (16.4-18.1 wt.%) contents remains broadly constant. They plot along a distinct evolutionary trend with higher SiO_2 contents at overlapping CaO and MgO contents relative to the IBT and IBT 'upper' glasses (Fig. 6).

The most voluminous UBT, corresponding to unit Bt13, likely results from numerous amalgamated depositional units, and was sampled directly above the Spiaggia Lunga (24 ky) marker bed at Grotta dei Pisani. Glass compositions of Bt13 extend to the most evolved products observed in the entire Vulcano UBT succession (58.1-63.3 wt.% SiO_2). Where Bt13 glasses overlap in SiO_2 content with the younger BT depositional units, the latter are typically dominated by glasses with higher K_2O content (e.g., Bt15; Fig. 6). The highest SiO_2 glasses observed within the Bt13 samples display the lowest CaO, FeOt and MgO contents within the entire UBT succession (Fig. 6). Stratigraphically higher in the Bt13 unit on Vulcano, above the Quadrara marker bed (21 ky), glasses are more restricted in their degree of evolution (VUL09/19; 56.1-59.3 wt.% SiO_2). Whilst, the uppermost portion of Bt13 on Vulcano (sample bt02/16), collected immediately below the Cugni di Molinello scoria bed, displays some of the least evolved compositions observed through the entire Bt13 unit (55.7-58.5 wt.% SiO_2).

The Cugni di Molinello scoria is a key marker bed within the UBT succession on Vulcano (Fig. 2). Here we present glass data for the Cugni di Molinello scoria to help assess their geochemical relationship. Glasses (*n = 19*) are relatively homogeneous trachy-andesites (52.3-54.3 wt.% SiO_2) with a K-series affinity (5.2-6.2 wt.% K_2O), and show most significant variability in their MgO (2.9-4.0 wt.%) and CaO (6.3-8.0 wt.%) contents (Fig. 6). The Cugni di Molinello scoria are more primitive than all the UBT deposits.

Above the Cugni di Molinello scoria bed, the UBT (Bt14) are quite homogenous (55.9-57.9 wt.% SiO_2) (Fig. 6). The Bt15 unit displays some of the most potassic glasses throughout the UBT macro-unit, with a dominant population containing ca. 7 wt.% K_2O. Juvenile glasses from both the Bt15 (56.3-60.7 wt.% SiO_2) and Bt16 (56.9-61.2 wt.% SiO_2) units are more heterogeneous than those of Bt14, and display some of the most evolved UBT glass compositions after the basal portions of the Bt13 unit (Fig. 6).

A minor, silicic, secondary glass component is identified in the Bt16 depositional unit sampled on Vulcano immediately above the Vallone del Gabellotto tephra erupted from Lipari. These secondary rhyolitic glasses (SiO_2 = 75.0 ± 0.3 wt.%; Na_2O + K_2O = 9.2 ± 0.5 wt.%; Fig. 5A) display a clear HKCA affinity (K_2O = 5.3 ± 0.5 wt.%; Fig. 5B). Also, two glass analyses (ca. 53 wt.% SiO_2) from the Bt14 unit are chemically consistent with the underlying Cugni di Molinello scoria (Fig. 6),

4.2.3.2 UBT units that outcrop on Lipari

The UBT on Lipari are sampled above the IBT ‘upper’, exclusively belonging to the Bt13 depositional unit. Overall the juvenile glasses sampled at Chiesa Vecchia (north Lipari) and Vallone Canneto Dentro (central-eastern) are broadly consistent, with a heterogeneous composition ranging from tephri-phonolites to trachytes (SiO_2 = 57.7-64.2; Na_2O + K_2O = 8.2-11.3 wt.%; *n = 63*; Fig. 5A) and a K-series affinity (K_2O = 5.1-7.1 wt.%; Fig. 5B). With increasing SiO_2 content these UBT juvenile glass display decreasing CaO (2.3-5.5 wt.%; Fig. 6B), FeOt (4.4 -6.7 wt.%), MgO (0.9-2.8 wt.%; Fig. 6C), TiO_2 (0.5-0.8 wt.%) and Al_2O_3 (15.5-17.7 wt.%) content, whilst K_2O content increases, and Na_2O (2.9-4.6 wt.%) remains broadly constant. In central-eastern Lipari, the juvenile glasses of the basal Bt13 unit (LIP09/19) are largely distinct from those overlying (LIP07/19), whereby the latter are typically offset to higher SiO_2 at overlapping CaO, MgO and K_2O contents (Fig. 6). The same compositional heterogeneity is shown by glasses of the Bt13 unit collected at Chiesa Vecchia (north Lipari). A secondary component of higher SiO_2 glasses (66.1-68.8 wt.%; *n = 7*) is observed in the upper sample of Bt13 sampled at Chiesa Vecchia (LIP03/19), recognised on the basis of a clear compositional gap (ca.64-66 wt.%; Fig. 6) which separates them from the dominant juvenile component.

5. DISCUSSION

Stratigraphic relationships and detailed geochemical characterization of the BT on Lipari and Vulcano are integrated to give constraints on their areal distribution and correlations with proximal near-source units. This provides the basis for proximal-medial-distal tephra correlations, and fundamental insights into hazard assessment in this active sector of the Aeolian Islands.

5.1 Geochemical characteristics of the BT volcanic glasses and a proximal link to Vulcano

Major and minor element glass geochemistry of the juvenile component of individual BT depositional units reveals that they are relatively homogeneous with K-series populations ranging from basaltic trachy-andesites, through trachy-andesites and tephri-phonolites, up to more evolved trachytes (Fig. 5A). The minor outlying HKCA rhyolitic glasses, and CA to HKCA andesite to dacite glasses recognized in some depositional units of the LBT, IBT and UBT are considered as “secondary” components, which do not reflect the juvenile magmas feeding the BT. Their origin is discussed in Section 5.2. Consequently, the overall compositional field of BT volcanic glasses is significantly more restricted when compared to the one proposed by Lucchi et al. (2008). A narrower compositional range centred exclusively around K-series volcanic glasses reinforces the correlation of the BT with the Vulcano magmatic system. During its intermediate to youngest stages of evolution, Vulcano has been the dominant source of K-series products within the Aeolian archipelago (Fig. 5A-C). The evolutionary trends observed here within the overall BT dataset are entirely consistent with the previously characterised near-source Vulcano volcanic glasses (Fig. 5C-D). Indeed, the only other source of K-series magmas within the archipelago, and similar to those of the BT, is the Stromboli volcano, specifically during the Neostromboli period (~13-4 ky; Francalanci et al., 2013; Albert et al., 2017; Fig. 5). An association between the BT and eruptive activity on Stromboli is, however, implausible owing to their greater thicknesses on Vulcano and Lipari relative to the rest of the archipelago (including Stromboli). Furthermore, K-Series activity on Stromboli is temporally incompatible with the longer-term emplacement of the BT succession. Finally, in terms of glass compositions, at overlapping SiO_2 content, the BT glasses display TiO_2 content more consistent with Vulcano products (lower-TiO_2) rather than those erupted on Stromboli (Fig. 5C). This final observation is pertinent when assessing the provenance of distal K-series marine tephra layers which might be related to the eruptions responsible for the BT.

Resolving unique geochemical fingerprints for the LBT and IBT glasses is a significant challenge given their large degree of chemical overlap. They are broadly consistent in terms of their SiO_2 content (~52-57 wt.%), and across most other major and minor elements (Fig. 8). Some subtle differences may offer potential to help provenance medial-distal equivalents of the BT deposits, particularly where chrono-stratigraphy is poorly constrained. The least evolved IBT glasses contain higher MgO, CaO and FeOt relative to those analysed throughout the LBT (Figs. 5 and 8). More useful is that the IBT glasses range to higher K_2O content than those of the LBT, thus at overlapping SiO_2, where K_2O content exceeds 6.3 wt.%, an attribution to the IBT is more likely (Fig. 7C).

The UBT glasses can be distinguished from those of the IBT (and LBT) owing to their higher SiO_2, trachy-andesitic to trachytic compositions (Fig. 5). The UBT glasses extend to lower TiO_2 contents compared to the underlying IBT units, again consistent with the overall trends observed in the glasses of known Vulcano erupted products (Fig. 5C). The UBT glasses also plot on subtly different evolutionary trends from those of the IBT, and this is well illustrated by CaO and MgO content plotted against SiO_2 (Fig. 6), where both CaO and MgO contents of the UBT extend to lower values than those of the IBT glasses (Fig. 6).

The stratigraphic boundary between the IBT and UBT macro-units had been previously defined by the identification of the widespread Monte Guardia tephra marker bed (Lucchi et al. 2008) and dated here at 25,920-27,025 cal y BP. The observed geochemical distinction between the IBT and UBT makes it possible to define a different geochemical-evolutionary boundary between the two successions. The lowermost depositional unit (Bt12) of the stratigraphically defined UBT macro-unit, immediately overlying the Monte Guardia tephra on both Vulcano (Gelso) and at various locations across Lipari (Fig. 6), is in fact chemically consistent with the IBT (those deposits beneath the Monte Guardia; Fig. 6), and consequently this depositional unit is re-defined in this study as the IBT '*upper*'. On Vulcano, the IBT/UBT chemical transition is observed relative to the Spiaggia Lunga scoria unit in the western sector of the island, whereby IBT type compositions are not observed in BT deposits above the Spiaggia Lunga, instead exclusively evolved UBT compositions are recognized. The age of 24 ± 5 ky for Spiaggia Lunga (Soligo et al., 2000) allows us to redefine the chronological boundary between IBT (56-24 ky) and UBT (24-8 ky). Unfortunately, where the Spiaggia Lunga scoria is not present, the IBT to UBT chemo-stratigraphic boundary is more difficult to identify, and this is the case on Lipari where no obvious unconformities are recognized at the corresponding stratigraphic level. However, charcoal dated from within the IBT 'upper' on Lipari is dated here at 25,800-26,190 cal y BP and this eruption age is in good chrono-stratigraphic agreement with the inferred Spiaggia Lunga boundary-transition age on Vulcano. The Spiaggia Lunga scoria unit crops out along the south-western border of the La Fossa caldera, which is the likely source area of the BT. Interestingly, Nicotra et al. (2020) have proposed that the emplacement of the Spiaggia Lunga scoria unit is directly linked to a volcano-tectonic (caldera) collapse event on Vulcano. It can be thus postulated that a collapse of the La Fossa caldera has coincided with a reconfiguration of this magmatic system, and the production of more evolved magmas which feed the UBT.

The more evolved depositional units that form the UBT (Bt13-16) show considerable compositional variability (Fig. 6). The most evolved glasses erupted within the UBT are associated with the most voluminous and oldest portion of Bt13, below the Cugni di Molinello scoria marker bed (Fig. 6). There is clear chemical overlap between the Bt13 depositional unit sampled on Vulcano and further north on Lipari. For instance the lowermost Bt13 samples from Vallone Canneto Dentro on Lipari (LIP09/19) are very consistent with the analysed deposits from the lowest portions of Bt13 on Vulcano. However, there are some noticeable spatio-chemical variations associated with unit Bt13. The remaining Lipari Bt13 samples (LIP07/19, LIP04/19 and LIP03/19) are dominated by glasses which reside on a subtly distinct evolutionary trend to those prevalent in the Vulcano deposits, this is best illustrated by a subtle offset to higher SiO_2 at overlapping K_2O, CaO and MgO content (Fig. 6). Importantly, from a correlation and provenance perspective, these higher SiO_2 glasses are also observed in the basal Bt13 deposit closer to source on Vulcano, albeit as a lower proportion of the glasses analyzed. Published data (sample VL328) stratigraphically equivalent to Bt13 reported on Vulcano (Lucchi et al. 2008) is also consistent with the data presented here from Lipari. The most obvious explanation for a lower proportion of higher SiO_2 UBT glasses in our Vulcano dataset is because our sampling concentrated at the top and bottom of the thick Bt13 depositional unit, whereby the intermediate portion was not analysed. In contrast on Lipari, further from vent, this depositional unit is thinner and more compact, for instance at Vallone Canneto Dentro the analyses appear to reveal a more heterogeneous Bt13 signature, with data reflecting both the subtly offset UBT evolutionary trends (Fig. 6). There is a return to less evolved trachy-andesite compositions (ca. 57 wt.%) in the uppermost portion of unit Bt13 (sample bt02/16), directly underlying the Cugni di Molinello scoria bed. This variability suggests that Bt13 does not represent a single depositional unit, but an amalgamation of lithologically homogeneous deposits, as also testified by the occurrence of localized erosional surfaces throughout the thickness of Bt13. The upper portion of Bt13 and Bt14 on Vulcano are indistinguishable in their composition, and are merely stratigraphically separated by the less evolved Cugni di Molinello scoria (Fig. 6), seemingly sourced from a separate vent within the La Fossa caldera (Dellino et al., 2011). Bt15 and Bt16 return to more evolved trachytic glass compositions, more consistent with those deposits from Bt13 (Fig. 6), making independent stratigraphic control important when distinguishing depositional units throughout the UBT. Bt15 is distinctive in terms of its prevalence of higher-K_2O glasses at overlapping SiO_2 content relative to other UBT deposits, a feature that is also apparent in published data from the same stratigraphic level (sample VL151; Lucchi et al. 2008).

5.2 The secondary glass compositions: insight into the BT depositional mechanisms

In addition to the dominant juvenile K-series glass components of the BT, a small proportion of chemical outliers are recognized in some depositional units of the LBT, IBT and UBT on both Vulcano and Lipari. These glasses are genetically unrelated to magmas feeding the eruptions responsible for the BT and are termed here as “secondary glasses”. HKCA rhyolitic glass compositions identified in some IBT and UBT units are entirely consistent with the silicic activities on Lipari during the past ca. 50 ka (Fig. 5A-B). Specifically, the rhyolitic glasses observed in the depositional units Bt8 and Bt9-10 of the IBT on Lipari, Bt12 of the newly defined IBT ‘upper’ on Lipari and Bt16 of the UBT on Vulcano. Lipari HKCA rhyolitic glasses can be most easily distinguished using their SiO_2 and K_2O content. On this basis we see that the rhyolitic glasses observed as secondary glasses can be compositionally linked to the pumice beds stratigraphically underlying each of the above-mentioned BT depositional units. The Bt8 and Bt9-10 depositional units of IBT contain high-SiO_2 (~76 wt.%) rhyolites with high K_2O (~5.5-6.2 wt.%), largely consistent with the underlying Falcone and Punta di Perciato tephra deposits related to eruptive activity in southern Lipari (Fig. 9A-B). There is also a degree of chemical overlap with rhyolitic glasses of the Lip1 tephra. This newly identified tephra layer separating the Bt9 and Bt10 depositional units, clearly documents a previously un-reported explosive eruption in the southern dome-field of Lipari given its glass composition spans those of the underlying (Falcone) and overlying (Monte Guardia) eruption units (Fig. 9A-B). The Bt12 (IBT 'upper') deposits across Lipari and in southern Vulcano (Gelso) contain minor components of high-SiO_2 rhyolites (~76 wt.%) with far more variable K_2O content (4.7-6.0- wt.%), consistent with the pumice and ash compositions of the underlying Monte Guardia eruption deposits (Fig. 9A-B). Whilst the HKCA rhyolitic glasses within the Bt16 unit of UBT on Vulcano are more consistent with the underlying Vallone del Gabellotto tephra deposits from Lipari (Fig. 9).

Similarly, CA to HKCA andesitic glass compositions are identified in the depositional units Bt3-4 of the LBT that outcrop on Lipari and are either interbedded within, or directly overly the GPT deposits from neighbouring Salina (Fig. 9, C-D). These glass compositions are entirely consistent with the GPT deposits characterised proximally on Salina (Sulpizio et al., 2016), but also include new glass data for the proximal GPT, and medial-distal occurrences sampled on Lipari (LIP41/17; SME4/5), Vulcano (VUL05/18) and Panarea (PAN07/17). The additional occurrence of basaltic-andesite to andesite glass compositions consistent with the GPT in the depositional units Bt1-2 of the LBT in western Lipari (Fig. 9C-D) is instead likely to be attributed to an underlying tephra deposit (reported as I1 tephra by Forni et al. 2013) which shares a similar composition to the products of the GPT (Fig. 9C-D).

Furthermore, unit Bt14 of the UBT on Vulcano contains a minor component of K-series glasses which are entirely consistent with the juvenile products of the underlying, more primitive, Cugni di Molinello scoria bed (Fig. 6).

The presence of a minor component of glass fragments within some BT depositional units that compositionally correlate to the underlying pyroclastic units is the result of clast-embedding, ripped up from the incoherent substratum by PDCs laterally spreading from the source area on Vulcano. This is clearly observed in the field where pumice and/or scoria from the underlying incoherent pyroclastic units are ripped-up and embedded at the base of the individual BT depositional units in the sampled outcrops, a feature first observed by Lucchi et al. (2008; 2013b). These authors suggested that PDC erosion and abrasion was limited to proximal to mid-proximal areas, whereas here we suggest that clast-embedding could be effective even at a greater distance up to at least the northern sector of Lipari (more than 10 km from the source).

5.3 BT links with proximal units on Vulcano

Here our volcanic glass dataset for the LBT, IBT and UBT is used to assess correlations with proximal units on Vulcano, to further constraint source/vent location. For this purpose we discuss the geochemical affinity of the LBT, IBT and UBT with the volcanic units belonging to the corresponding chrono-stratigraphic windows that currently outcrop along the borders of the La Fossa caldera, which have been considered as the most probable BT source area (Lucchi et al., 2008, 2013b). Lucchi et al. (2008, 2013b) established a univocal lithostratigraphic correlation between the UBT and the Piano Grotte dei Rossi Tuffs, which are best exposed along the south-eastern rim of La Fossa caldera, in the area of Il Piano and crop out discontinuously on western and southern Vulcano. These show a regular decrease of deposit thickness from the caldera rim towards southern Vulcano that indicate an origin from a (undefined) vent within the La Fossa caldera.

Instead, there remains a challenge in defining correlations and areal distributions of the LBT-IBT (80-24 ky) because deposits with their typical lithofacies are absent in the area of Il Piano, given the UBT stratotype is observed here, it should represent the main depositional area of the LBT-IBT units, assuming that their source area has not changed over time. In this area, the MM1-3 pyroclastic successions occupy the chrono-stratigraphic window corresponding to the LBT-IBT (in addition to other minor units). Specifically, the MM1-2 are found interlayered between Vulcano products dated at 78-77 ky and 53-48 ky, which broadly corresponds to the 80-56 ky chrono-stratigraphy of the LBT, whilst the IBT (56-24 ky) are more likely to correspond to the MM3 that is loosely defined in the stratigraphic interval above 53-48 ky and the UBT (<24 ky). In addition to a compatible chrono-stratigraphic position, the MM1-3 share many lithological and textural features with the LBT-IBT deposits, consisting of massive ash with discontinuous lamination and planar to inclined bedding, with abundant clinopyroxene crystals and internal banding of colour and grain-size. Furthermore, distinctive black to yellowish scoria lapilli of MM3 are recognized in a number of stratigraphic positions within the IBT including at Grotta dei Pisani and Gelso on Vulcano, or along the southern sector of Lipari. These lines of evidence were responsible for Lucchi et al. (2008, 2013b) proposing that the MM1-3 could represent the near source counterpart of the LBT-IBT units. However, a clear lithostratigraphic correlation between the LBT-IBT units and the MM1-3 has not yet been established, and thus geochemical support becomes particularly important.

The K-series basaltic trachy-andesitic, tephri-phonolitic and trachy-andesitic glasses of the LBT and IBT are indeed broadly consistent with the volcanic glasses erupted during the emplacement of the proximal MM1-3 (Fig. 7-8). Our samples and subsequent glass analyses, reported in Supplementary A, are unlikely to be representative of the full compositional variability of these thick eruptive successions, particularly owing to the poor preservation of the hydrothermally altered MM3 deposits. Regardless of this, the MM1 glasses show some overlap with both the LBT and IBT, although they are dominated by subtly more evolved glass compositions, particularly with respect to those LBT-IBT on Lipari (Fig. 8). There is significant geochemical overlap between the LBT and MM2 glasses (Fig. 8), whilst the IBT appear to show subtle offsets, for instance MM2 glasses do not fully satisfy the higher K_2O (Fig. 7C) or lower TiO_2 observed in the IBT glasses. Whilst a link between the MM1 and the earliest LBT cannot be completely excluded, an assignment of the MM2 as a near-source counterpart of the LBT on Vulcano seems the most probable, consistent with the reconstructed chrono-stratigraphy. Indeed, the correlation is also supported by the occurrence of a layer of grey pumice lapilli (VUL05/18) observed within the MM2 (Fig. 4; sec. 2 on Vulcano). These lapilli display glass compositions consistent with those of the GPT from Salina, which critically is also found interlayered within the LBT on Lipari (Fig. 9), Salina and Panarea (See Section 5.4).

Coarse proximal MM3 scoria fall (sample BT03/20), along with the more evolved component of a black to yellowish MM3 scoria fall deposits traced to southern Vulcano (Gelso; VUL04/17), are consistent with the IBT (Fig. 7-8). The proximal MM3 (BT03/20) glasses are chemically consistent with the least evolved ash deposits of the IBT observed on both Vulcano and Lipari (Fig. 8), while the most evolved scoria (54.4 wt.% SiO_2) analysed displays higher K_2O, and lower CaO and MgO content consistent with the dominant IBT glass compositions (Fig. 8D-F). These proximal MM3 scoria fall (BT03/20) also shows broad chemical consistency with the scoria fall identified within the IBT on Lipari (Fig. 8), albeit these MM3 glasses are offset to higher K_2O content (Fig. 7C). MM3 fall sampled in southern Vulcano (Gelso) is bimodal, while one population is more primitive (~ 49 wt.% SiO_2) than the IBT deposits, the second is chemically consistent with the IBT glasses, even extending to the same more elevated K_2O contents, and further supporting a link between the MM3 and the IBT (Fig. 7C; 8D-F). Combining the proximal and medial MM3 scoria fall data reveals a substantial compositional variability, and this variability appears to correspond to a significant proportion of overall IBT chemical variability observed. However some of the more evolved IBT glass compositions are not satisfied by the available MM3 data, and again this is likely to reflect MM3 preservation related sampling biases. Both in terms of limited stratigraphic coverage of the proximal MM3 succession sampled, and the associated difficulties of being able to chemically compare the same lithofacies. For instance, proximal MM3 alternates between scoria fall and ash-rich PDC deposits, here we are only able to analyse the fresh scoria fall, whilst the IBT characterised clearly relate to PDCs. Overall, there is sufficient chemical agreement to support the chrono-stratigraphic link between the MM3 and the IBT.

Our geochemical dataset shows that the juvenile UBT glasses (trachy-andesites to trachytes) are very similar to glass compositions of the early to intermediate products of La Fossa cone, namely the Punte Nere and Grotta dei Palizzi deposits (Fig. 6). Interestingly, volcanic glasses of the Punte Nere pyroclastic succession can be chemically distinguished and lie on separate evolutionary trends (Fig. 6). The lowermost Punte Nere (VUL01/17) deposits, and ultimately the earliest La Fossa products recognized in the volcanic stratigraphy, are entirely consistent with the UBT (Fig. 6). Whilst these lowermost Punte Nere deposits are slightly more evolved than the products of the youngest UBT depositional unit (Bt16), they are entirely consistent with the older Bt13 deposits sampled across Vulcano and Lipari, and the Bt15 deposits (Fig. 6). This geochemical link is important given that the Punte Nere pyroclastics are massive to cross-laminated, dark grey ash deposits, lithologically very similar to UBT, yet direct stratigraphical relationships between the two successions are lacking in the field (Fig. 2). The geochemical similarity between the UBT and the earliest Punte Nere products suggests that the UBT may be associated with the earliest activities of the La Fossa cone too, probably sharing the same magmatic plumbing system. It is even plausible that some of the older Punte Nere products recognized in the field may actually equate to the uppermost UBT. Either way this outlines a direct relationship between the UBT and the active La Fossa cone which was not fully demonstrated by previous studies, and illustrates a possible continuity in the evolution of the magmatic and eruptive system of La Fossa cone starting (at least) from the onset of UBT activity at ~24 ky, which extends its life cycle.

As highlighted, the glass compositions within the basal Punte Nere succession are variable. Whilst the oldest Punte Nere deposits (VUL01/17), are chemically consistent with the UBT, the overlying Punte Nere glasses analysed (VUL02/17; VUL03/17) are offset in terms of their CaO, MgO and K_2O content (Fig. 6). Interestingly, these glasses, and those of the younger Grotta dei Palizzi successions (cf. Albert et al., 2012), lie on the same evolutionary trends as the older IBT glasses, albeit extending to more evolved end-member (Fig. 6). Our heterogeneous Punte Nere data, which are consistent with published Punte Nere and Grotta dei Palizzi glass data (Fig. 6), suggest that the La Fossa explosive activity at this time was fed by a complex magmatic system comprising of more than one magma batch

5.4 Proximal-medial-distal correlations

5.4.1 BT occurrences on Salina, Panarea, Filicudi and Capo Milazzo (Sicily)

Here we use new glass analyses (Supplementary Material B) of BT occurrences from across the Aeolian archipelago (Salina, Filicudi and Panarea) and Capo Millazzo (Sicily) to help constrain the dispersal of volcanic ash associated with the successive eruptions on Vulcano. Considerable geochemical overlap between the juvenile glass components of the LBT and IBT macro units (Section 5.1) means that correlations rely on the stratigraphic context at individual localities throughout the Aeolian islands, and often relying upon key stratigraphic markers beds (e.g., the Ischia Tephra or GPT).

BT depositional units observed on Salina underlying the Ischia tephra in the stratigraphic window of the LBT have relatively homogeneous glass chemistries that overlap with the glasses of the LBT elsewhere, and the proximal MM1-2 on Vulcano (Fig. 7B; Fig. 8A-C). These LBT deposits observed on Salina lack secondary glass components from the underlying strata, coherent with their occurrence on the lava flows related to the final activity of Monte dei Porri stratocone dated at 67-57 ky (Lucchi et al. 2013a) and the absence of significant abrasion effects.

Ash deposits chemically consistent with the LBT and IBT are recognised on Panarea and these are attributed to the former owing to the presence of GPT from Salina interbedded within (Fig. 7B; 8A-C). Deposits with relatively homogeneous glasses consistent with the LBT also outcrop on Capo Milazzo peninsula (Fig. 7B; 8A-C), although without the stratigraphic constraints coming from other tephra marker beds, a link to the IBT cannot be excluded. This highlights the importance of external chrono-stratigraphic markers, or dating (^{14}C) to constrain the timing of the source eruptions on Vulcano and their associated ash dispersals.

K-series ash deposits on Filicudi island (FIL07/18), northwest of Vulcano, are entirely consistent with the LBT and IBT glass compositions (Fig 7C; Fig. 8D-F). However, based on their stratigraphic position above the Ischia tephra these deposits are firmly attributed to the activity of the IBT. A second Filicudi ash unit (FIL08/18) is also interpreted as IBT based on its position above the Ischia tephra and its glass compositions being broadly consistent with the most evolved IBT (Fig. 8D-F).

5.4.2 Possible BT occurrences in the sedimentary records of the Central Mediterranean

Given their significant near-source thickness on Vulcano and Lipari and wide distribution throughout the Aeolian Islands (Salina, Panarea and Filicudi), the successive BT depositional units potentially represent the source equivalents of volcanic ash layers recorded in sedimentary archives (marine and lacustrine) across the Central Mediterranean. The region has a well-established distal tephrostratigraphic framework (e.g., Keller et al., 1978; Paterne et al., 1988, Calanchi and Dinelli 1998; Wulf et al., 2004; Sulpizio et al., 2010; Giaccio et al., 2017) with many widespread ash layers tied into the well-dated eruption stratigraphies of the productive central Mediterranean volcanoes, particularly those in Campania (e.g., Campi Flegrei, Ischia). Therefore, the identification of BT deposits within this tephrostratigraphic framework would not only provide information on the distribution and scale of explosive activity on Vulcano, it also offers chronological constraints on the timing of eruptions on the island. With some exceptions, the presence of BT deposits in regional sedimentary archives is largely underexplored (e.g. Paterne et al., 1988; Calanchi et al., 1994; Di Roberto et al., 2008; Albert et al., 2012; Tamburrino et al., 2016), probably due to an inadequate knowledge of their stratigraphy, and most importantly their geochemical (juvenile glass) signatures, essential to reliable source attributions. Here we use our extensive volcanic glass dataset to evaluate the distribution and timing of distal BT occurrences.

In the chrono-stratigraphic window of the LBT (80-56 ky), Tyrrhenian (and Adriatic) Sea marine cores, including those investigated by Paterne et al. (1986; 1988), do not reveal any obvious ash layers candidates for distal LBT in the deep-sea realm. In terms of IBT and UBT occurrences, Tamburrino et al. (2016) explored the ash deposits preserved in the Marsili Basin core, MD01-2474G (Fig. 1a), situated on a topographic high. They proposed the possible occurrence of ash layers associated with the IBT (MD27, MD22, MD15) and UBT (MD11 and MD3) eruptions, although it is worth noting that these correlations were made in the absence of reliable BT reference glass data. Albert et al. (2012) reported the occurrence of ‘pre-La Fossa’ Vulcano tephra (TIR2000-50cm) in another Marsili Basin core, TIR2000-C01 (Fig. 1a), situated more than 20 km ENE of the Stromboli Canyon mouth, a major source of volcaniclastic material into the Basin. The Marsili Basin captures volcaniclastic turbidites relating to pyroclastic material deposited on the islands, and directly into the marine environment, consequently we carefully re-evaluate the available data from these Marsili cores. Unfortunately, with TIR2000-C01, the age of ash layers below the Soccavo 1 tephra (Campi Flegrei) at ~ 12 ky (TIR2000-93cm) were not well constrained in the absence of reliable chrono-stratigraphic or biostratigraphic markers. Conversely, the Marsili core MD01-2474G has a more reliable chronology developed using radiocarbon dating, and orbitally-tuned chronological tie-points (Tamburrino et al., 2016). Broad agreement exists between the independent chronology of the record and the preferred ages of key chrono-stratigraphic markers, particularly those in the deeper portion of the core. For instance, layer MD28 (54.8 ky) correlates to the widespread marine ash layer, the Y-7, equivalent to the Ischia Tephra, dated at 56.1 ± 1.0 ky (Giaccio et al., 2017), thus providing a direct tie-point between the onland BT stratigraphy and the marine core. Furthermore, our GPT (Salina) glass data corroborates its distal occurrence in MD01-2474G (MD33 [58.9 ky]; Fig. 9C-D), offering another terrestrial-marine chrono-stratigraphic tie point. Crucially, co-located tephras in the Marsili cores now facilitate the transfer of age information from MD01-2474G to TIR2000-CO1.

The oldest ash layer in MD01-2474G, MD27, previously linked to the IBT (Tamburrino et al., 2016), comprises a dominant component of transitional HKCA/SHO trachy-andesitic glasses. This layer is dated using the cores age-model at 42.7 ky, an age which is further corroborated by the presence of a secondary Pantellerite glass shards linked to the Pantelleria Green Tuff (Tamburrino et al., 2016) that is $^{40}Ar/^{39}Ar$ dated at 45.7 ± 1.0 ky ([95.4%]; Scaillet et al., 2013). Compared to our juvenile BT data it is apparent that these SHO glasses are generally too low in K_2O content, and too high in TiO_2 to be associated with IBT activity on Vulcano (Fig. 10). Glass data indicates they reside on an evolutionary trend more akin to glasses erupted on Stromboli during the Paleostromboli epoch, rather than the central sector of the Aeolian archipelago..

Ash layer MD22 (MD01-2474G) dated at 36.9 ky was linked to the IBT (Tamburrino et al., 2016), our data clearly indicate that this layer is inconsistent with the IBT the and Vulcano magmatic system (Fig. 10). Tamburrino et al. (2016) linked this 8.3 cm thick tephra deposit to a layer in TIR2000-C01, namely TIR2000-417 cm. Here we suggest that there is better chemical agreement between MD22 and the overlying tephra in TIR2000-C01, TIR2000-

398cm, a 20 cm thick coarse-grained volcaniclastic turbidite (Di Roberto et al., 2008; Albert et al., 2012). MD22 appears to contain both chemical components of the TIR2000-398cm deposit (Fig. 10), the transitional CA/HKCA glasses which extend from basaltic-andesites through andesites and dacites, to a low-SiO_2 rhyolites (Component-1), and HKCA basaltic-andesites (Component-2). This clear chronological tie-point between MD01-2474G and TIR2000-C01 means we can import the MD01-2474G age of 36.9 ky to the TIR2000-398cm tephra unit. This offers useful chronology to the basal sediments of TIR2000-C01, critical when assessing the age of other ash deposits in this core. The sedimentological features of MD22/TIR2000-398cm, including grain-size and layer thickness, combined with the different chemical arrays observed, indicate this deposit is linked with a major volcanic collapse. The data from this deposit are clearly inconsistent with Vulcano and the central sector of the Aeolian archipelago. The high TiO_2 content of the glasses (Fig. 10B) may prompt future investigations of a link to one of the many collapse events to have occurred on Stromboli island (Francalanci et al., 2013).

MD15 (29.7 ky) in MD01-2474G, a 10.8 cm thick tephra, was linked to IBT activity on Vulcano, its trachy-andesitic glasses are transitional between HKCA/SHO (Tamburrino et al., 2016). Importantly these glasses display lower K_2O content than the IBT volcanic glasses at overlapping SiO_2 content, and more elevated TiO_2 content is again inconsistent with the BT and Vulcano (Fig. 10). Two trachy-andesite ash layers, MD11 (16.7 ky) and MD3 (6.9 ky), in the MD01-2474G core were attributed to the 'Tufi di Grotte dei Rossi inferiori', here equivalent to the UBT (Tamburrino et al., 2016). Whilst both layers display glasses that overlap with those of the UBT, they show more elevated TiO_2 content at particular SiO_2 contents, which is again more consistent with Stromboli than the UBT and Vulcano (Fig. 10B).

Returning to Marsili core TIR2000-C01, in light of new age constraints, with 36.9 ky placed on the coarse-grained volcaniclastic turbidite (CGVT; TIR2000-398cm = MD22), we are able to evaluate the timing of potential distal BT deposits found in the core stratigraphically above this CGVT. Between the Campi Flegrei tephra Soccavo 1 (TIR2000-93cm) found at 93 cm depth in TIR2000-C01, and the CGVT (TIR2000-398) at 398 cm a crude sedimentation rate of 12.4 cm/ky^{-1} is calculated. This is a noticeable increase from a rate of 7.72 cm/ky^{-1} observed in the upper portion of the core between the 776 CE Monte Pilato tephra from Lipari (TIR2000-7cm), found at depth of 7 cm, and the Soccavo 1 (TIR2000-93cm). However, given the frequent occurrence of volcaniclastic turbidity current deposits (Di Roberto et al., 2008), a highly variable sedimentation rate is expected; indeed, such variability was also recognised in Marsili core MD01-2474G (Tamburrino et al., 2016). Without calculating an event-free sedimentation rate, our TIR2000-C01 tephra age estimates are tentative.

Many ash rich, volcaniclastic turbidites within TIR2000-C01 have not been chemically characterised (Di Roberto et al., 2008; Albert et al., 2012), here we provide new glass data from some which reinforce the occurrence of marine deposits chemically consistent with the BT in the Marsili Basin, and highlight the need for future investigations of similar sedimentary successions from the southern Tyrrhenian Sea. A thin (3 mm) ash deposit sampled at a depth of 297 cm, TIR2000-297cm, has a homogeneous K-Series (Fig. 10), basaltic trachy-andesite to trachy-andesite affinity, with an age of ~28.7 ky. The glass compositions are generally consistent with the eruptive products of the IBT on Lipari, and in particular the diffuse scoria fall (LIP27/17; Fig. 8D-F) observed in the depositional unit above the Falcone dome (~43-40 ky), although we must acknowledge a subtle offset in FeOt content (Fig. 8F). With an age of ~28.7 ky for TIR2000-297cm we tentatively suggest this marine tephra pre-dates the widespread 25,885-27,055 cal y BP Monte Guardia eruption, and therefore it is plausible that the tephra relates to IBT activity preserved on Lipari Island between the local Falcone and Monte Guardia tephra beds (Bt10 or Bt11).

Stratigraphically higher in the TIR2000-C01 succession, a thin (2 mm) ash rich tephra, TIR2000-160cm, has a relatively heterogeneous (57.4-61.4 wt.% SiO_2) K-series (Fig. 10), trachy-andesite to trachyte compositions with an age of ~16.7 ky. These glasses are entirely consistent with the UBT on Vulcano, whilst restricted by a limited number of analyses the compositional variability and chrono-stratigraphic position means a link to the eruptions responsible for Bt13 is most likely (Fig. 6). This marine tephra reinforces a chemical link to the La Fossa magmatic system deeper in time.

The K-series trachytic tephra TIR2000-50 (Fig. 10) has an age of ~6.7 ky, and its origin was the focus of previous debate. Di Roberto et al. (2008) initially attributed this layer to a collapse during the Secche di Lazzaro eruption on Stromboli (Neostromboli epoch). However, chemical investigations revealed that this tephra was actually more consistent with the eruptive products of Vulcano (Albert et al., 2012; 2017). Based on the diagnostic lower TiO_2 content of these volcanic glasses they were akin to the evolutionary trend of Vulcano products and thus suggested pre- or early La Fossa activity (Fig. 10B). Interestingly, the dominant K-series glasses are consistent with the UBT (Fig. 10A), whilst a secondary glass component of HKCA rhyolites are consistent with those of the Vallone del Gabellotto

(Lipari). This feature is consistent with the onland Bt16 depositional unit, immediately overlying the Vallone del Gabellotto (8.7–8.4 ky) tephra on Vulcano. A correlation of TIR2000-50cm to Bt16 would be consistent with the chrono-stratigraphy given the marine tephra deposits age (~6.7 ky). The overlying TIR2000-46cm unit is compositionally indistinguishable from the dominant K-series component of the underlying TIR2000-50 (Fig. 10), although this younger tephra (~6.1 ky) has no secondary rhyolitic component. It is plausible that this tephra also relates to the Bt16, and would imply that Bt16 depositional unit is the product of more than one eruption. These correlations give us new age constraints for the youngest portion of the UBT on Vulcano, which post-date the 8.5 ky (radiocarbon) age obtained by De Astis et al. (1997b).

Away from the Marsili Basin, two noticeable distal occurrences of potential IBT are worthy of discussion. The E-10 Tyrrhenian Sea ash layer preserved in KET8003 north of Salina (Fig. 1a) and dated to 35.2 ky (Paterne et al., 1988) appears to have a glass chemistry (Fig. 10) and chrono-stratigraphic position consistent with the IBT positioned between the Falcone and Monte Guardia tephra deposits outcropping on Lipari. Whilst Matthews et al. (2015) reported a basaltic trachy-andesite tephra, T1567, dated at between 35,693-34,064 cal y BP in the Southern Adriatic (core SA03-11; Fig. 1a) and positioned immediately above the 40 ky Campanian Ignimbrite (Y-5/C-13) tephra. The glass compositions of this tephra are entirely consistent with those of the IBT, and specifically to the diffuse scoria fall observed in the IBT above the 43-40 ky Falcone dome on Lipari (LIP27/17; LIP15/18; LIP16/18). The chrono-stratigraphy of this correlation is compelling and indicates a widespread ash fall event associated with the IBT at ~35 ky. Whilst there are clear chemical differences between the E-10 and T1567, their ages (~ 35 ky) are entirely compatible, indicating that the two distal tephra layers may reflect either; (1) closely spaced eruptions or eruptive phases on Vulcano, which cumulatively form part of the IBT eruptive cycle; or (2) different eruptive processes during the same IBT eruption. According to this hypothesis, the E-10 (Tyrrhenian Sea) marine tephra, which is chemically compatible with the IBT emplaced from PDCs across Lipari at this time, may relate to ash fall from a co-PDC plume. While in contrast T1567 (Adriatic Sea), is compositionally consistent with a phase of scoria fall embedded within these PDC deposits on Lipari and perhaps reflects ash dispersed from a quasi-sustained eruptive column. This would be consistent with the observed lithological features of the IBT and their likely proximal counterpart in Vulcano, the MM3, which are characterized by ash layers from PDCs, alternated with scoria lapilli fall.

6. CONCLUSIONS

Revised stratigraphic investigations combined with new radiocarbon ages and a large dataset of grain-specific volcanic glass compositional data for the different depositional units of the ash-rich Brown Tuffs (BT) on Lipari and Vulcano provide constraints on their large-scale correlations across the Aeolian archipelago and the southern Tyrrhenian Sea, along with insights for hazard assessments. The main outcomes of this work are the following:

(1) Juvenile BT eruptive material displays relatively homogeneous glass compositions, particularly in the case of individual depositional units. Overall these units range from basaltic trachy-andesites and trachy-andesites to trachytes, broadly evolving through the succession, with the most evolved glass compositions observed in the UBT macro unit. The LBT (80-56 ky) and IBT (56-24 ky) macro units are most challenging to chemically distinguish, with alkali variability most diagnostic. While the UBT macro unit can be distinguished on the basis that their glasses display higher SiO_2 and extend to lower TiO_2, CaO, MgO and FeOt contents.

(2) Secondary glass compositions within some of the BT depositional units are related to a minor component of embedded pumice and/or scoriae from the underlying incoherent pyroclastic units during the emplacement of the PDCs that deposited the BT in proximal-medial areas.

(3) The time interval of the eruptions that deposited the UBT has been re-defined to between 24 and 6 ky based on the observed chemo-stratigraphic transitions which coincides with the age of the Spiaggia Lunga marker bed on Vulcano, and thus replaces the older previously adopted Monte Guardia stratigraphic marker.

(4) Correlations between the LBT, IBT and UBT macro-units and proximal units on Vulcano are proposed, providing a more robust framework for the long-term hazard assessment related to explosive activity within the La Fossa Caldera. A clear geochemical link is suggested between the UBT and the early products of the La Fossa cone, suggesting a shared magmatic system during the last 24 ky, and thus extending the life cycle of this currently active eruptive source area.

(5) Unequivocal evidence that ash deposits preserved across the Aeolian archipelago and in Tyrrhenian and Adriatic Sea marine cores are chemically consistent with the IBT and UBT erupted on Vulcano offers important insights into the scale of these eruptions and the associated hazards.

Acknowledgements:

SM funded through a PhD Scholarship of the University of Bologna-Alma Mater Studiorum. PGA is funded through a UKRI Future Leaders Fellowship (MR/S035478/1). We thank Gianfilippo De Astis and another Anonymous Reviewer for their constructive comments.

REFERENCES

Albert, P.G., Tomlinson, E.L., Smith, V.C., Di Roberto, A., Todman, A., Rosi, M., Marani, M., Muller, W., Menzies, M.A., 2012. Marine-continental tephra correlations: volcanic glass geochemistry from the Marsili Basin and the Aeolian Islands, Southern Tyrrhenian Sea, Italy. J. Volcanol. Geotherm. Res. 229-230, 74-94.

Albert, P.G., Tomlinson, E.L., Smith, V.C., Di Traglia, F., Pistolesi, M., Morris, A., Donato, P., De Rosa, R., Sulpizio, R., Keller, J., Rosi, M., Menzies M., 2017. Glass geochemistry of pyroclastic deposits from the Aeolian Islands in the last 50 ka: a proximal database for tephrochronology. J. Volcanol. Geotherm. Res. 336, 81-107.

Barberi, F., Gasparini, P., Innocenti, F., Villari, L., 1973. Volcanism of the Southern Tyrrhenian Sea and its geodynamic implications. J. Geophys. Res. 78, 5221-5232.

Beccaluva, L., Gabbianelli, G., Lucchini, F., Rossi, P.L., Savelli, C., 1985. Petrology and K/Ar ages of volcanics dredged from the Aeolian Seamounts: implications for geodynamic evolution of the southern Tyrrhenian basin. Earth Planet. Sci. Lett. 74, 187-208.

Bergeat, A., 1899. Die Äolischen Inseln (Stromboli, Panaria, Salina, Lipari, Vulcano, Filicudi und Alicudi), Abh. Math. Phys. Kl. Kgl. Bayer. Akad. Wiss., vol. 20 I. Abt., München, 274.

Biass, S., Scaini C., Bonadonna C., Folch A., Smith, K., Höskuldsson, A., 2014. A multi-scale risk assessment for tephra fallout and airborne concentration from multiple Icelandic volcanoes-part 1: hazard assessment. Nat. Hazards Earth Syst. Sci. discuss. 2, 2463-2529.

Bonasia, R., Costa, A., Folch A., Macedonio, G., Capra, L., 2012. Numerical simulation of tephra transport and deposition of the 1982 El Chichón eruption and implications for hazard assessment. J. Volcanol. Geotherm. Res. 231-232, 39-49.

Brock F., Higham T., Ditchfield P. and Ramsey C. B. (2010) Current Pretreatment Methods for AMS Radiocarbon Dating at the Oxford Radiocarbon Accelerator Unit (ORAU). Radiocarbon 52, 103–112.

Bronk Ramsey, C. (2009). Bayesian analysis of radiocarbon dates. Radiocarbon, 51(1), 337-360.

Caron, B., Siani, G., Sulpizio, R., Zanchetta, G., Paterne, M., Santacroce, R., Tema, E., Zanella, E., 2012. Late Pleistocene to Holocene tephrostratigraphic record from the Northern Ionian Sea. Mar. Geol. 311-314, 41-51.

Calanchi, N., Gasparotto, G., Romagnoli, C., 1994. Glass chemistry in volcaniclastic sediments of ODP Leg 107, Site 650, sedimentary sequence: provenance and chronological implications. J. Volcanol. Geotherm. Res. 60, 59-85.

Calanchi, N., Cattaneo, A., Dinelli, E., Gasparotto, G., Lucchini, F., 1998. Tephra layers in Late Quaternary sediments of the central Adriatic Sea. Marine Geology 149, 191-209.

Chiarabba, C., De Gori, P. & Speranza, F. 2008. The Southern Tyrrhenian Subduction Zone: deep geometry, magmatism and Plio-Pleistocene evolution. Earth and Planetary Science Letters, 268, 408–423.

Cicchino, A., Zanella, E., De Astis, G., Lanza, R., Lucchi, F., Tranne, C.A., Airoldi, G., Mana S., 2011. Rock magnetism and compositional investigation of Brown Tuffs deposits at Lipari and Vulcano (Aeolian Islands – Italy) J. Volcanol. Geotherm. Res. 208, 23-28.

Crisci, G.M., De Rosa, R., Lanzafame, G., Mazzuoli, R., Sheridan, M.F., Zuffa, G.G., 1981. Monte Guardia Sequence: a Late-Pleistocene Eruptive Cycle on Lipari (Italy). Bull. Volcanol. 44, 241-255.

Crisci, G.M., Delibrias, G., De Rosa, R., Mazzuoli, R., Sheridan, M.F., 1983. Age and petrology of the Late-Pleistocene Brown Tuffs on Lipari, Italy. Bull. Volcanol 46, 381-391.

Crisci, G.M., De Rosa, R., Esperanca, S., Mazzuoli, R., Sonnino, M., 1991. Temporal evolution of a three component system: the island of Lipari (Aeolian Arc, southern Italy). Bull. Volcanol. 53, 207-221.

De Astis, G., Frazzetta, G. & La Volpe, L., 1989. I depositi di riempimento della caldera del Piano ed i depositi della Lentia. Bollettino GNV 2, 763-778.

De Astis, G., Dellino, P., De Rosa, R., La Volpe, L., 1997. Eruptive emplacement mechanism of fine grained pyroclastic deposits widespread on Vulcano Island. Bull. Volcanol. 59, 87-102.

De Astis, G., Ventura, G., Vilardo, G., 2003. Geodynamic significance of the Aeolian volcanism (Southern Tyrrhenian Sea, Italy) in light of structural, seismological, and geochemical data. Tectonics 22 (4), 1-17.

De Astis, G., Lucchi, F., Dellino, P., La Volpe, L., Tranne, C.A., Frezzotti, M.L., Peccerillo, A., 2013. Geology, volcanic history and petrology of Vulcano (central Aeolian archipelago). Geological Society, London, Memoirs 37, pp. 281–348.

Dellino, P., De Astis, G., La Volpe, L.,Mele, D., Sulpizio, R., 2011. Quantitative hazard assessment of phreatomagmatic eruptions at Vulcano (Aeolian Islands, Southern Italy), as obtained by combining stratigraphy, event statistics and physical modelling. J. Volcanol. Geotherm. Res. 201, 264-384.

De Rosa, R., Donato, P., Scarciglia, F., 2016. On the origin and post-depositional history of widespread massive ash deposits: the case of Intermediate Brown Tuffs (IBT) of Lipari (Aeolian Islands, Italy). J. Volcanol. Geotherm. Res. 327, 135-151.

Dingwell, A. and Rutgersson, A., 2014. Estimating volcanic ash hazard in European airspace. J. Volcanol. Geotherm. Res., 286, 55-66.

Di Roberto, A., Rosi, M., Bertagnini, A., Marani, M.P., Gamberi, F., Del Principe, A., 2008.

Deep water gravity core from the Marsili Basin (Tyrrhenian Sea) records Pleistocene-Holocenic explosive events and instabilities of the Aeolian Island Archipelago, (Italy). J. Volcanol. Geotherm. Res. 177 (1), 133-144.

Ellam, R.M., Hawkesworth, C.J., Menzies, M.A., Rogers, N.W., 1989. The volcanism of southern Italy: role of subduction and relationship between potassic and sodic alkaline magmatism. J. Geophys. Res. 94, 4589-4601.

Forni, F., Lucchi, F., Peccerillo, A., Tranne, C.A., Rossi, P.L., Frezzotti, M.L., 2013. Stratigraphic and geological evolution of the Lipari volcanic complex (central Aeolian archipelago). Geological society, London, Memoirs 37, 213-279.

Francalanci, L., Taylor, S.R.,McCulloch,M.T.,Woodhead, J.D., 1993. Geochemical and isotopic variations in the calc-alkaline rocks of Aeolian arc, southern Tyrrhenian Sea, Italy: constraints on magma genesis. Contrib. Mineral. Petrol. 113, 300-313.

Francalanci, L., Lucchi, F., Keller, J., De Astis, G., Tranne, C.A., 2013. Eruptive, volcano-tectonic and magmatic history of the Stromboli volcano (north-eastern Aeolian archipelago). Geological Society, London, Memoirs 37, 397-471.

Giaccio, B., Hajdas, I., Isaia, R., Deino, A., Nomade, S., 2017. High-precision 14C and 40Ar/39Ar dating of the Campanian Ignimbrite (Y-5) reconciles the time-scales of climatic-cultural processes at 40 ka. Sci. Rep. 7.

Jochum, K.P., Stoll, B., Herwig, K., Willbold, M., Hofmann, A.W., Amini, M., Aarburg, S., Abouchami, W., Hellebrand, E., Mocek, B., Raczek, I., Stracke, A., Alard, O., Bouman, C., Becker, S., Dücking, M., Brätz, H., Klemd, R., de Bruin, D., Canil, D., Cornell, D., de Hoog, C., Dalpé, C., Danyushevsky, L., Eisenhauer, A., Gao, Y., Snow, J.E., Groschopf, N., Günther, D., Latkoczy, C., Guillong, M., Hauri, E., Höfer, H.E., Lahaye, Y., Horz, K., Jacob, D.E., Kasemann, S.A., Kent, A.J.R., Ludwig, T., Zack, T., Mason, P.R.D., Meixner, A., Rosner, M., Misawa, K., Nash, B.P., Pfänder, J., Premo, W.R., Sun, W.D., Tiepolo, M., Vannucci, R., Vennemann, T., Wayne, D., Woodhead, J.D., 2006. MPI-DING reference glasses for in situ microanalysis: 581 New reference values for element concentrations and isotope ratios. Geochemistry Geophysics Geosystems 7(2).

Keller, J., 1967. Alter und Abfolge der vulkanischen Ereignisse auf den Äolischen Inseln Bericht Naturforschenden Gesellschaft Freiburg 57, 33-67.

Keller, J., 1980a. The island of Salina. Rendiconti della Società Italiana di Mineralogia e Petrologia 36, 489-524.

Keller, J., 1980b. The Island of Vulcano. Rendiconti della Società Italiana di Mineralogia e Petrologia 36, 369-414.

Keller, J., 1981. Quaternary tephrochronology in the Mediterranean region. In: Self, S. & Sparks, S. R. J. (eds) Tephra Studies. NATO, Advanced Study Institutes Series C 75, D. Reidel Publishing Company, Dordrecht, 227-244.

Kraml, M., Keller, J., Henjes-Kunst, F., 1997. Dating of Upper Quaternary deep-sea sediments from the Ionian Sea (Eastern Mediterranean) with laser 40Ar/39Ar analyses on prominent tephra layers. EUG 9 (European Union of Geosciences), Strasbourg (France) 23–27 March 1997, Terra Nova 9, Abstract Supplement 1, 406.

Insinga, D.D., Tamburrino, S., Lirer, F., Vezzoli, L., Barra, M., De Lange, G.J., Tiepolo, M., Vallefuoco, M., Mazzola, S., Sprovieri, M., 2014. Tephrochronology of the astronomically- tuned KC01B deep-sea core, Ionian Sea: insights into the explosive activity of the Central Mediteranean area during the last 200 ka. Quat. Sci. Rev. 85, 63-84.

Leocat, E., 2011. Histoire eruptive des volcans du secteur occidental des Iles Eoliennes (Sud de la Mer Tyrrhenienne, Italie). PhD thesis, University of Paris 11, Orsay.

Le Pennec, J.L., Ruiz, G.A., Ramón, P., Palacios, E., Mothes, P., Yepes, H., 2012. Impact of tephra falls on Andean communities: The influences of eruption size and weather conditions during the 1999-2001 activity of Tungurahua volcano, Ecuador. J. Volcanol. Geotherm. Res. 217-218, 91-103.

Losito, R., 1989. Stratigrafia, caratteri deposizionali e aree sorgente dei tufi bruni delle Isole Eolie. Unpublished PhD Thesis, University of Bari, Italy.

Lucchi, F., 2013. Stratigraphic methodology for the geological mapping of volcanic areas: insights from the Aeolian archipelago (southern Italy). Geol. Soc. Lond. Mem. 37,37–53.

Lucchi, F., Tranne, C.A., De Astis, G., Keller, J., Losito, R., Morche, W., 2008. Stratigraphy and significance of Brown Tuffs on the Aeolian Islands (southern Italy). J. Volcanol. Geotherm. Res. 177, 49-70.

Lucchi, F., Gertisser, R., Keller, J., Forni, F., De Astis, G., Tranne, C.A., 2013a. Eruptive history and magmatic evolution of the island of Salina (central Aeolian archipelago). Geological Society, London, Memoirs 37, 155-211.

Lucchi, F., Keller, J., Tranne, C., 2013b. Regional stratigraphic correlations across the Aeolian archipelago (southern Italy). Geological Society, London, Memoirs 37, 55-81.

Lucchi, F., Tranne, C.A., Peccerillo, A., Keller, J., Rossi, P.L., 2013c. Geological history of the Panarea volcanic group (eastern Aeolian archipelago). Geological Society, London, Memoirs 37, 349-393.

Lucchi, F., Peccerillo, A., Tranne, C. A., Rossi, P. L., Frezzotti, M. L. & Donati, C. 2013d. Volcanism, calderas, and magmas of the Alicudi composite volcano (western Aeolian archipelago). Geological Society, London, Memoirs, 37, 83–111.

Lucchi, F., Santo, A.P., Tranne, C.A., Peccerillo, A., Keller, J., 2013e. Volcanism, magmatism, volcano-tectonics and sea-level fluctuations in the geological history of Filicudi (western Aeolian archipelago). Geological Society, London, Memoirs 37, 113-153.

Machida, H., 1999. The stratigraphy, chronology and distribution of distal marker tephras in and around Japan. Global and Planetary Change 21, 71-94.

Manetti, P., Pasquaré, G., Tibaldi, A., Tsegaye, A., 1988. Geology of the island of Filicudi (Aeolian arc). Bollettino G.N.V. IV, 368-382.

Manetti, P., Pasquaré, G., Tibaldi, A., Tsegaye, A., 1995. A new geo-vulcanological map of Filicudi island (Aeolian arc, Italy). Acta Vulcanologica 7, 1-5.

Martin, R.S., Watt, S.F.L., Pyle, D.M., Mather, T.A., Matthews, N.E., Georg, R.B., Day, J.A., Fairhead, T., Witt, M.L.I., Quayle, B.M., 2009. Environmental effects of ashfall in Argentina from the 2008 Chaitén volcanic eruption. J. Volcanol. Geotherm. Res. 184, 462-472.

Matthews, I.P., Trincardi, F., Lowe, J.J., Bourne, A.J.,MacLeod, A., Abbott, P.M., Anderson, N., Asioli, A., Blockley, S.P.E., Lane, C.S., Oh, Y.A., Satow, C.S., Staff, R.A.,Wulf, S., 2015. Developing a robust tephrochronological framework for Late Quaternary marine records in the Southern Adriatic Sea: new data from core station SA03-11. Quat. Sci. Rev. 118, 84-104.

Morche, W., 1988. Tephrochronologie der Aolischen Inseln. (Unpublished PhD Thesis). Albert-Ludwigs-Universitat Freiburg, Germany.

Narcisi, B., 1996. Tephrochronology of a late quaternary lacustrine record from the Monticchio maar (Vulture volcano, southern Italy). Quaternary Science Review 15, 155-165.

Paterne, M., Guichard, F., Labeyrie, J., Gillot, P.Y., Duplessy, J.C., 1986. Tyrrhenian Sea tephrochronology of the oxygen isotope record for the past 60,000 years. Mar. Geol. 72, 259-285.

Paterne, M., Guichard, F., Labeyrie, J., 1988. Explosive activity of the South Italian volcanoes during the past 80,000 years as determined by marine tephrochronology. J. Volcanol. Geotherm. Res. 34, 153-172.

Peccerillo, A., De Astis, G., Faraone, D., Forni, F., Frezzotti, M.L., 2013. Compositional variation of magmas in the Aeolian arc: implications for petrogenesis and geodynamics.Geological Society, London, Memoirs, 489-508.

Pichler, H., 1980. The Island of Lipari. Rendiconti della Società Italiana di Mineralogia e Petrologia 36, 415-440.

Ramsey C. B., Higham T. F. G. and Leach P. (2004) Towards high-precision AMS; progress and limitations. Radiocarbon 46, 17–24.

Reimer, P., Austin, W., Bard, E., Bayliss, A., Blackwell, P., Bronk Ramsey, C., Butzin, M., Cheng, H., Edwards, R., Friedrich, M., Grootes, P., Guilderson, T., Hajdas, I., Heaton, T., Hogg, A., Hughen, K., Kromer, B., Manning, S., Muscheler, R., Palmer, J., Pearson, C., van der Plicht, J., Reimer, R., Richards, D., Scott, E., Southon, J., Turney, C., Wacker, L., Adolphi, F., Büntgen, U., Capano, M., Fahrni, S., Fogtmann-Schulz, A., Friedrich, R., Köhler, P., Kudsk, S., Miyake, F., Olsen, J., Reinig, F., Sakamoto, M., Sookdeo, A., & Talamo, S. (2020). The IntCal20 Northern Hemisphere radiocarbon age calibration curve (0–55 cal kBP). Radiocarbon, 62.

Scaillet, S., Vita-Scaillet, G., Rotolo, S.G., 2013. Millennial-scale phase relationships between ice-core and Mediterranean marine records: insights from high-precision 40Ar/39Ar dating of the Green Tuff of Pantelleria, Sicily Strait Quat. Sci. Rev. 78, 141-154.

Scaini, C., Biass, S., Galderisi, A., Bonadonna, C., Folch, A., Smith, K., Hoskuldsson, A., 2014. A multi-scale risk assessment for tephra fallout and airborne concentration frommultiple Icelandic volcanoes-part 2: vulnerability and impact. Nat. Hazards Earth Syst. Sci. Discuss. 2, 2531-2595.

Shane, P., 2000. Tephrochronology: a New Zealand case study. Earth-Science Reviews 49, 223-259.

Siani, G., Sulpizio, R., Paterne, M., Sbrana, A., 2004. Tephrostratigraphy study for the last 18,000 14C years in a deep-sea sediment sequence for the South Adriatic. Quat. Sci. Rev. 23, 2485-2500.

Soligo, M., De Astis, G., Delitala, M.C., La Volpe, L., Tadderucci, A., Tuccimei, P., 2000. Disequilibri nella serie dell uranio nei prodotti dell isola di Vulcano: cronologia isotopica e implicazioni magmatologiche. 2 Forum Italiano di Scienze della Terra Riassunti, Plinus. 22, 347-349.

Sulpizio, R., Zanchetta, G., D'Orazio, M., Vogel, H., Wagner, B., 2010. Tephrostratigraphy and tephrochronology of lakes Ohrid and Prespa, Balkans. Biogeosciences 7, 3273-3288.

Sulpizio, R., Folch, A., Costa, A., Scaini, C., Dellino, P., 2012. Hazard assessment of far-range volcanic ash dispersal from a violent Strombolian eruption at Somma-Vesuvius volcano, Naples, Italy: implications on civil aviation. Bull. Volcanol. 74, 2205-2218.

Sulpizio, R., Zanchetta, G., Caron, B., Dellino, P., Mele, D., Giaccio, B., Insinga, D., Paterne, M., Siani, G., Costa, A., Macedonio, G., Santacroce, R., 2014. Volcanic ash hazards in the Central Mediterranean assessed from geological data. Bull. Volcanol. 76, 866.

Sulpizio, R., Forni, F., Lucchi, F., Massaro, S., Tranne, C., 2016. Unravelling the effusive-explosive transitions and the construction of a volcanic cone from geological data: the example of Monte dei Porri, Salina Island (Italy). Journal of Volcanology and Geothermal Research 327, 1-22.

Tamburrino, S., Insinga, D.D., Pelosi, N., Kissel, C., Laj, C., Capotondi, L., Sprovieri, M., 2016. Tephrochronology of a ~ 70 ka-long marine record in the Marsili basin (southern Tyrrhenian Sea) J. Volcanol. Geotherm. Res. 327, 23-39.

Tomlinson, E.L., Albert, P.G.,Wulf, S., Brown, R., Smith, V.C., Keller, J., Orsi, G., Bourne, A.J., Menzies, M.A., 2014. Age and geochemistry of tephra layers from Ischia, Italy: constraints from proximal-distal correlations with Lago Grande di Monticchio. J. Volcanol. Geotherm. Res. 287, 22-39.

Ventura, G., 2013. Kinematics of the Aeolian volcanism (Southern Tyrrhenian Sea) from geophysical and geological data. In: Lucchi, F., Peccerillo, A., Keller, J., Tranne, C. A. & Rossi, P. L. (eds) The Aeolian Islands Volcanoes. Geological Society, London, Memoirs 37, 3-11.

Wulf, S., Kraml, M., Brauer, A., Keller, J. & Negendank, J. F. W. 2004. Tephrochronology of the 100 ka lacustrine sediment record of Lago Grande di Monticchio (southern Italy). Quaternary International 122, 7-30.

Zanchetta, G., Sulpizio, R., Roberts, N., Cioni, R., Eastwood, W., Siani, G., Caron, B., Paterne, M., Santacroce, R., 2011. Tephrostratigraphy, chronology and climatic events of the Mediterranean basin during the Holocene: An overview. Holocene 21, 33-52.

CAPTIONS

Fig. 1. Sketch maps of the islands of Vulcano, Lipari, Salina, Filicudi and Panarea (Aeolian archipelago) and the Capo Milazzo in northern Sicily showing the outcrop areas of the BT. The inset (a) shows the location of the Aeolian Islands and seamounts in the southern Tyrrhenian sea (depth contour lines in metres below sea level). Coordinates conform to the Gauss-Boaga System (IGM). The sites of marine cores TIR200-C01 (Albert et al., 2012), KET8003 (Paterne et al., 1988), MD01-2474G (Tamburrino et al., 2016) and SA03-11 (Matthews et al., 2015), that have BT units, are also outlined.

Fig. 2. Generalized stratigraphic correlations of the BT successions and age constraints in the study area. The most complete BT succession is recognized on the island of Lipari, subdivided into several depositional units (Bt1-16) superposed to the LBT, IBT and UBT macro-units by means of interlayered volcanic units and tephra layers, erosive surfaces and reworked horizons. The Bt12 depositional unit immediately overlying the Monte Guardia tephra is considered as part of the IBT (namely IBT 'Upper') following the chemical evidence presented here (whilst it was part of the UBT macro unit as defined by Lucchi et al., 2008). The LBT, IBT and UBT are then correlated with distinct sectors of the island of Vulcano, the islands of Salina, Filicudi, Panarea and the Capo Milazzo peninsula. Please note that the recognized depositional units are a minimum number as some lithologically-homogeneous units could have be amalgamated. References for the stratigraphic units in the different sites are: Forni et al., 2013 (Lipari); De Astis et al., 2013 (Vulcano); Lucchi et al., 2013a (Salina); Lucchi et al., 2013e (Filicudi); Lucchi et al., 2013c (Panarea); Morche, 1988 (Capo Milazzo). The Lip1 and Lip2 tephras are described in Table 1, whilst 'ext' is an external tephra not discussed here. On Salina, the Sal III and Sal IV tephra layers (Lucchi et al., 2008 and references therein) are correlated with tephra layers C(i)-8 and C(i)-7 in the Tyrrhenian sea core KET 8011 (Paterne, 1985; Paterne et al., 1988). Some additional tephra layers interlayered within the BT succession (not displayed here) provide stratigraphic boundaries between distinct depositional units of BT (not correlated between the islands), and based on their glass geochemistry they are likely to correlate with widespread central Mediterranean isochronous markers derived from the Campanian volcanic zone and recorded in marine and lacustrine successions.

Fig. 3. Field evidence and main sampling outcrops of the BT on Lipari and Vulcano. A) Vallone Canneto Dentro, central-eastern Lipari: LBT and IBT macro-units with interlayered Grey Porri Tuffs (gpt), Ischia Tephra (it) and the local Punta di Perciato (pe), Falcone (fa)

and Monte Guardia pumice pyroclastics (gu). B) Valle Muria, south-western Lipari: IBT interlayered with the local Punta di Perciato (pe), Falcone (fa) and Monte Guardia pumice pyroclastics (gu). C) Canneto, eastern Lipari: IBT 'upper' (see the text for explanation) and UBT above the Monte Guardia marker bed (gu). D) Vallone Canneto Dentro, central-eastern Lipari: IBT 'upper' and UBT above the Monte Guardia marker bed (gu), bounded at the top by the local Vallone Cannetro Dentro (cd) pumice succession. E) Vallone Fiume Bianco, central-northern Lipari: top portion of the UBT interlayered between the local Vallone del Gabellotto (vg) and Monte Pilato (mp) pumice successions. F) Grotta dei Pisani, western Vulcano: UBT located above the Spiaggia Lunga scoria marker bed. G) Grotta dei Pisani, western Vulcano: IBT and LBT below the Spiaggia Lunga scoria marker bed (sl), characterized by massive ash deposits alternated with scoria lapilli layers (*). H) Il Piano, central Vulcano: Monte Molineddo 1, 2, 3 (mm3) pyroclastic successions outcropping in the stratigraphic window of the LBT and IBT.

Fig. 4. Correlation of selected stratigraphic sections showing the main sampled outcrops of the BT on Lipari and Vulcano (the scale is only approximate). Labels for the shown stratigraphic units: pv=Paleo-Vulcano, sl=Spiaggia Lunga, ma=Monte Aria; mm1=Monte Molineddo 1, mm2=Monte Molineddo 2, mm3=Monte Molineddo 3, mr=Monte Rosso, pp=Passo del Piano, qd=Quadrara, cm=Cugni di Molinello, sa=Monte Saraceno, pn=Punte Nere, gp=Grotta dei Palizzi, co=marine deposits, lf='leaf-bearing pyroclastics', gpt=Grey Porri Tuffs, it=Ischia-Tephra, pe=Punta di Perciato, fa1=Falcone pumice, fa2=Falcone domes, lip1=lip1 tephra, exl=external tephra (not discussed here), lpt=Lower Pollara Tuffs, gu=Monte Guardia, lip2=lip2 tephra, cd=Vallone Canneto dentro, vg=Vallone del Gabellotto, rw=reworked horizon. References for the stratigraphic units herein are Forni et al., 2013 (Lipari) and De Astis et al., 2013 (Vulcano).

Fig. 5. Major element (wt.%) glass geochemical variations of the BT glasses analysed in this study compared to the volcanic glasses of explosive eruption deposits produced on Vulcano, Lipari, Salina and Stromboli during the last 50 ky. (A) TAS classification diagram of BT glasses, also shown are the compositional ranges of the whole rock (WR) data for Vulcano, Lipari, Salina and Stromboli; (B) SiO_2 vs K_2O classification diagram; (C) SiO_2 vs. TiO_2 diagnostic plot used for distinguishing the potassic eruptive products of Vulcano and Stromboli, and illustrating the BT clear link to volcanism on Vulcano and useful when considering the provenance of distal marine tephra layers; (D) MgO vs. CaO plot further illustrating that the BT juvenile glasses conform to the compositions of eruptive products known to have been produced on Vulcano (including the Quadrara Formation, Casa Lentia,

Grotta dei Palizzi 1 and 2, Caruggi formation/Breccia di Commenda, Lower and Upper Pietre Cotte). Error bars represented 2*standard deviations of replicated analyses of the StHs6/80-G secondary standard glass run alongside the BT samples. References: (1) Albert et al., 2017; (2) De Astis et al., 2013; (3) Forni et al., 2013; (4) Francalanci et al., 2013; and (5) Lucchi et al., 2013a.

Fig. 6. Major element (wt.%) glass geochemical variation diagrams (A-C) showing the different UBT depositional units sampled on Vulcano and Lipari (D). Shown are the compositions of the newly defined IBT 'upper' which immediately overly the Monte Guardia tephra at various outcrops on Lipari and Vulcano (Gelso). These deposits are re-classified as the IBT 'upper' owing to their chemical similarity to the IBT found below the Monte Guardia marker bed. A minor secondary components of more evolved trachyte is shown within the Bt13 (LIP03/19) deposits at Chiesa Vecchia, Lipari and these share a similar chemical affinity to the explosive products of the Casa Lentia eruptive succession on Vulcano. HKCA rhyolitic secondary glass component are also observed in Bt16 on Vulcano, these are not shown here, instead refer to Figure 9. New glass data is presented for the Cugni di Molinello scoria bed which is interbedded between the Bt12 and Bt13 depositional units on Vulcano, these more primitive fall out scoria deposit are also believed to derive from activity within the La Fossa caldera, albeit erupted from a separate vent area to the UBT (Dellino et al., 2011). Glass data collected from a marine ash sample TIR2000-160cm taken from the Marsili Basin marine core is also shown to have a clear UBT affinity. Error bars represented 2*standard deviations of replicated analyses of the StHs6/80-G secondary standard glass run alongside the BT samples. References: (1) Lucchi et al., 2008 and (2) Albert et al., 2017.

Fig. 7. Major element glass geochemical variation diagrams for the juvenile component of the LBT, IBT and IBT 'upper' outcropping on Lipari and Vulcano compared to near-vent deposits on Vulcano and distal tephra layers. The near-vent eruption deposits on Vulcano considered responsible for the LBT and IBT are Monte Molineddo 1-3. Also shown are the proximal deposit of the younger Punte Nere succession and the Cugni di Molinello (CM). Here more distal occurrences of the LBT and IBT units focus on deposits found outcropping across the archipelago on Salina, Panarea, Filicudi and Capo Milazzo (Sicily). The similarity between fallout components of the IBT deposits and a distal marine tephra layers in the Tyrrhenian (Paterne et al., 1988) and Adriatic Seas (Matthews et al., 2015) is explored. (A) TAS classification diagram of LBT and IBT glasses, (B, C) SiO_2 vs K_2O classification diagrams of the LBT and IBT deposits and distal equivalents. Error bars represented

2*standard deviations of replicated analyses of the StHs6/80-G secondary standard glass run alongside the BT samples.

Fig.8. Major element glass geochemical variation diagrams for the juvenile component of the LBT, IBT and IBT 'upper' outcropping on Lipari and Vulcano compared to near-vent deposits on Vulcano and distal tephra layers found on the neighboring islands and in the marine setting. LBT are considered in the context of Monte Monlineddo 1 and 2 units on Vulcano, whilst the IBT are compared to the limited glass data available for the Monlineddo 3 unit. Error bars represented 2*standard deviations of replicated analyses of the StHs6/80-G secondary standard glass run alongside the BT samples.

Fig. 9. Major element geochemical variability diagram of the secondary glass components found within a selection of BT depositional units outcropping primarily on Lipari, but also Vulcano. These minor populations are chemically related to the underlying stratigraphic units which were subject to clast embedding and erosion processes. Error bars represented 2*standard deviations of replicated analyses of the StHs6/80-G secondary standard glass run alongside the BT samples.

Fig. 10. Major element geochemical variability of the BT deposits compared to marine tephra deposits considered here to be related to the BT eruption units, or have been previously ascribed as distal BT deposits in the literature. (A) SiO_2 vs K_2O classification diagram; (B) SiO_2 vs. TiO_2 diagnostic plot used for distinguishing the potassic eruptive products of Vulcano and Stromboli, and very useful when considering the provenance of distal marine tephra layers associated with the two islands. Error bars represented 2*standard deviations of replicated analyses of the StHs6/80-G secondary standard glass run alongside the BT samples. TIR2000 Marsili Basin cores samples are from Albert et al. (2012) and Albert (2012); the MD Marsili Basin marine tephra layers are from Tamburrino et al. (2016), the marine layers E-11 (Tyrrhenian Sea) and T1567 (Adriatic) are reported in Paterne et al. (1988) and Matthews et al. (2015) respectively.

Table 1

Main characteristics of tephra layers and marker beds used for the subdivisions of BT depositional units and correlations (listed in stratigraphic order starting from the older one). Recognition area: Str=Stromboli, Pan=Panarea, Sal=Salina, Lip=Lipari, Vul=Vulcano, Fil=Filicudi, Ali=Alicudi; Mil=Capo Milazzo. Chemical composition of juvenile glass fragments (w.r=whole rock) is reported by referring to: (1) present work; (2) Albert et al (2017); (3) De Astis et al 2013: CA=calcalkaline, HKCA=high-k calcalkaline, SHO=shoshonite series; Bas=basalt, Bas-And=basaltic andesite, And=andesite, Dac=dacite, Rhy=rhyolite, Lat=latite, Sho=shoshonite, Tra=trachyte). Correlations with proximal stratigraphic units refer to: (1) Lucchi et al. (2008); (2) Forni et al. (2013); (3) Lucchi et al., 2013a; (4) De Astis et al. 2013. Age references: (1) Morche, 1988; (2) De Astis et al 1989; (3) Soligo et al 2000; (4) Siani et al., 2004; (5) Leocat, 2011; (6) Lucchi et al., 2013a, b; (7) Sulpizio et al. 2016; (8) Giaccio et al. 2017; (9) present work.

Tephra	Marine tephra	Lithology	Dispersal area	Chemistry (glass)	Source area	Proximal stratigraphic unit	Age (ky)
Grey Porri Tuff		Grey (to whitish) scoria and pumice lapilli and ash	Sal, Lip, Pan, Mil	CA Bas-And to Dac	Sal	Rocce di Barcone Fm. (3)	70–67 (1,6,7)

		Grey fine to coarse ashes, with abundant mm-sized cpx crystals and interlayered yellowish scoriaceous lapilli	Vul		Vul	M. Molineddo 1 (4)	
		Varicoloured ash, locally with beds of scoriaceous lapilli and isolated bombs	Vul		Vul	M. Molineddo 2 (4)	
Ischia Tephra	Y-7	White-yellowish ash	Str, Pan, Sal, Lip, Fil	Tra-Pho (1)	Ischia	Epomeo Green Tuff –Monte Sant'Angelo (1)	56.1±1.0 (8)
		Black to yellowish scoriaceous lapilli and bombs and grey coarse to fine ashes with abundant mm-sized euhedral cpx crystals	Vul		Vul	M. Molineddo 3 (4)	
Punta di Perciato		Whitish pumice lapilli and ash	Lip	Rhy (1)	Lip	Punta di Perciato Fm., member pe_2 (2)	
Falcone		Whitish pumice lapilli and ash	Lip	Rhy (1)	Lip	Falcone Fm., member fa_1 (2)	43-40 (5)
lip1		Whitish ash	Lip	Rhy (1)	Lip		
Lower Pollara Tuff		Lapilli and ash of yellow pumice and black scoria	Sal, Lip	CA- to HKCA Bas-And to And	Sal	Punta Fontanelle Form. (3)	27.6-26.4 (9)
Monte Guardia		White and grey pumice (and obsidian) lapilli and ash	Lip, Vul, Sal, Pan	Rhy (1,2)	Lip	Monte Guardia Fm. (2)	27-26 (9)
Spiaggia Lunga		Red to black scoria lapilli and bombs	Vul	SHO Bas to Sho (w.r.) (3)	Vul	Spiaggia Lunga Fm. (4)	24±5 (3)
Cugni di Molinello		Black scoria lapilli	Vul	Sho	Vul	Cugni di Molinello Fm. (4)	
lip2		Pumice and obsidian lapilli and ash	Lip	Rhy (1)	Lip		
Monte Saraceno		Red to black scoria lapilli	Vul	Sho (w.r.) (3)	Vulc	Monte Saraceno Fm., member sa_1 (4)	8.3±1.6 (2)
Vallone Canneto dentro		Pumice and obsidian lapilli and ash	Lip	Rhy (1)	Lip	Vallone Canneto dentro Fm., member cd_1 (2)	
Vallone del Gabellotto	E-1	White pumice ash and lapilli	Lip, Pan, Vul, Str	Rhy (1,2)	Lip	Vallone del Gabellotto Fm. (2)	8.7 – 8.4 (4)
Punte Nere		Dark grey lapilli and ash	Lip	Tra-Pho (1)	Vul	Punte Nere Fm., member pn_1 (4)	5.3 +2.2/-1.1 (3)

Table 2

Radiocarbon age determinations of charcoals sampled from within the BT succession and the palaeosol overlying the UBT. (A) Radiocarbon age determinations presented here from between the Monte Guardia Tephra and the Vallone Cannetto Dentro on Lipari Island. Charcoal LIP14/17 was collected at Location 9 (Fig. 3) and LIP07/17 was collected at Location 8 (Fig. 3). Ages are calibrated using IntCal20 (Reimer et al., 2020) and OxCal v4.4. Calibrated age-distribution plots are provided in supplementary information A. (B) Radiocarbon ages from the literature recalibrated using IntCal20 (Un-modelled), while some of the age determinations have been incorporated into an Bayesian age-depth model which is used to provide new age constraints on the Monte Guardia and Lower Pollara eruption deposits used as chrono-stratigraphic markers in the Aeolian Islands. Detaiils of the Bayesian age model are reported in Supplementary Material A. * Age range represents 82.2% probability, with 8.7% probability range of 5325-5390 cal y BP.

Eruption Unit	Location	Sample ID	Material	Oxford Lab Code	^{14}C age	Error (68.2%)	$\delta^{13}C$	cal y BP (95.4%; IntCal20) (Un-modelled)			cal y BP (95.4%; IntCal20) Modelled Age			Reference
(A) This study														
IBT *Upper*	Lipari	LIP014/17	Charcoal	OxA-36000	20020	90	-24,83	23830	-	24240	23830	-	24260	This Study
IBT *Upper*	Lipari	LIP07/17	Charcoal	OxA-35999	21760	100	-24,73	25845	-	26310	25830	-	26295	This Study
(B) Re-calibrated published data + Bayesian Modelling														
-	*Lipari*		palaesol (bulk Sed)	-	4810	60	-	5445*	-	5610*	-		-	Pichler, 1980
UBT	Vulcano		Charcoal	-	7680	100	-	8305	-	8655	-	-	-	De Astis et al., 1997
UBT	Lipari	-	Charcoal	-	16800	200	-	19825	-	20845	-	-	-	Crisci et al., 1983
IBT *Upper*	Lipari		Charcoal	-	20500	200	-	24155	-	25200	24240	-	25240	Crisci et al., 1983
IBT *Upper*	Lipari		Charcoal	-	20300	700	-	22950	-	26005	24110	-	25980	Crisci et al., 1983
Monte Guardia (mg)											25920	-	27025	This Study
IBT	Lipari		Charcoal	-	22480	1100	-	24570	-	29500	26125	-	27295	Crisci et al., 1983
IBT	Lipari		Charcoal	-	22600	300	-	26100	-	27460	26300	-	27275	Crisci et al., 1981
Lower Pollara Tuff (lpt)											26425	-	27585	This Study
IBT	Lipari		Charcoal	-	22940	340	-	26445	-	27770	26575	-	27760	Morche, 1988
IBT	Lipari		Charcoal	-	23500	900	-	26085	-	29850	26495	-	28100	Crisci et al., 1983

Table 3

Average of major and minor element composition of juvenile glass of selected Lower and Intermediate Brown Tuffs units included in the study. Totals are pre-normalised analytical totals. n = number of analyses used to calculate the average. Locality is referred to Fig.4. A complete geochemical dataset is provided in Supplementary material B.

Macro Unit	LOWER BROWN TUFF													
Locality	1 (Lipari)		8 (Lipari)		8 (Lipari)		1 (Lipari)		8 (Lipari)		8 (Lipari)		1 (Vulcano)	
Unit	bt 1		bt 1/2		bt 3		bt 4		bt 4		bt 6		?	
Sample	bt06/16 (L) 2φ		LIP10/18 3φ		LIP05/18 3φ		bt09/16 (L) 3φ		LIP04/18 3φ		LIP02/18 3φ		VUL10/18 3φ	
Material	ash		ash		ash		ash		ash		ash		ash	
n	10		10		11		8		19		11		16	
	mean	1σ	mean	1σ	mean	1σ	mean	1σ	mean	1σ	mean	1σ	mean	1σ
(wt%)														
Total	96.83	1.50	96.70	0.60	97.07	1.80	97.57	1.11	97.66	1.40	98.19	0.78	98.66	1.15
SiO_2	54.68	0.80	54.01	0.62	56.68	0.33	56.13	0.42	53.76	0.49	53.41	0.93	56.77	1.10
TiO_2	0.99	0.03	0.84	0.10	0.87	0.07	0.99	0.09	0.79	0.05	0.73	0.11	0.97	0.05
Al_2O_3	16.58	0.13	17.03	0.63	16.44	0.38	16.39	0.20	17.55	0.38	17.78	0.91	16.35	0.37
FeO	9.22	0.61	8.63	0.64	8.18	0.38	8.83	0.35	8.03	0.26	8.02	1.08	8.15	0.56
MnO	0.21	0.05	0.19	0.03	0.20	0.04	0.22	0.04	0.16	0.02	0.17	0.05	0.16	0.03
MgO	2.76	0.37	2.83	0.17	2.13	0.20	2.29	0.26	2.69	0.15	2.78	0.39	2.09	0.38
CaO	6.09	0.64	6.24	0.26	5.38	0.21	5.54	0.40	6.02	0.28	6.23	0.67	5.22	0.68
Na_2O	3.61	0.25	4.19	0.32	3.89	0.23	3.57	0.45	4.50	0.25	4.43	0.74	3.97	0.25
K_2O	5.10	0.58	5.16	0.37	5.33	0.23	5.16	0.22	5.66	0.25	5.63	0.49	5.47	0.45
P_2O_5	0.61	0.05	0.69	0.04	0.66	0.07	0.68	0.04	0.68	0.03	0.70	0.09	0.67	0.03
Cl	0.15	0.02	0.20	0.04	0.23	0.07	0.19	0.06	0.15	0.03	0.12	0.03	0.18	0.05

Macro Unit	INTERMEDIATE BROWN TUFF													
Locality	2 (Lipari)		4 (Lipari)		10 (Lipari)		6 (Lipari)		6 (Lipari)		2 (Lipari)		1 (Vulcano)	
Unit	bt 7		bt 9		bt 8/9		bt 9		bt 10		bt 11		?	
Sample	bt11/16 (L)		LIP14/18 3φ		LIP45/17		LIP27/17		LIP36/17 -1φ		bt15/16 (L) 2 φ		VUL09/18 2φ	
Material	ash		ash		scoria		scoria		ash		ash		ash	
n	10		27		10		18		20		10		10	
	mean	1σ	mean	1σ	mean	1σ	mean	1σ	mean	1σ	mean	1σ	mean	1σ
(wt%)														
Total	97.46	1.27	96.19	0.91	98.59	0.74	97.01	1.18	98.16	0.62	97.83	1.28	99.07	0.83
SiO_2	54.77	0.45	54.17	0.57	51.15	0.69	53.61	0.54	53.85	0.40	54.44	0.41	55.12	0.32
TiO_2	0.83	0.05	0.77	0.05	0.77	0.07	0.90	0.03	0.82	0.05	0.75	0.05	0.85	0.05
Al_2O_3	17.21	0.40	17.25	0.36	17.22	0.48	17.17	0.17	17.02	0.27	17.35	0.26	16.59	0.31
FeO	8.24	0.29	8.14	0.37	9.34	0.52	8.68	0.29	8.64	0.27	8.21	0.32	8.65	0.20
MnO	0.18	0.05	0.20	0.04	0.19	0.04	0.18	0.06	0.19	0.06	0.21	0.06	0.19	0.04
MgO	2.20	0.29	2.19	0.17	4.21	0.59	3.05	0.24	2.60	0.31	2.09	0.16	2.29	0.05
CaO	5.31	0.56	5.38	0.23	8.86	0.87	6.92	0.43	5.88	0.45	5.25	0.36	5.52	0.14
Na_2O	4.00	0.35	4.75	0.17	3.72	0.32	3.95	0.28	4.20	0.18	4.27	0.31	4.17	0.18
K_2O	6.26	0.49	6.02	0.16	3.88	0.53	4.65	0.27	5.87	0.34	6.46	0.47	5.61	0.18
P_2O_5	0.75	0.05	0.83	0.06	0.49	0.08	0.60	0.04	0.73	0.05	0.71	0.03	0.73	0.02
Cl	0.25	0.04	0.31	0.03	0.17	0.02	0.29	0.02	0.20	0.04	0.25	0.04	0.28	0.02

Table 4

Average of major and minor element composition of juvenile glass of selected Upper-Intermediate and Upper Brown Tuffs units included in the study. Totals are pre-normalised analytical totals. n = number of analyses used to calculate the average. Locality is referred to Fig.4. A complete geochemical dataset is provided in Supplementary material B.

Macro Unit	INTERMEDIATE BROWN TUFF 'UPPER'				
Locality	7 (Lipari)	12 (Lipari)	9 (Lipari)	13 (Lipari)	3 (Vulcano)

Unit	bt 12		bt 12		bt 12		bt 12		bt 12	
Sample	bt01/16 (L) 3 φ		LIP18/17 1φ		LIP06/17 -1φ		LIP21/17 -1φ		VUL09/17 1φ	
n	11		17		26		24		10	
	mean	1σ	mean	1σ	mean	1σ	mean	1σ	mean	1σ
(wt%)										
Total	97.10	1.26	97.73	0.64	97.18	0.96	97.88	0.61	97.83	0.97
SiO_2	54.55	0.68	54.26	0.62	54.89	0.38	54.73	0.42	54.09	0.49
TiO_2	0.78	0.05	0.71	0.03	0.71	0.03	0.73	0.05	0.72	0.05
Al_2O_3	17.48	0.14	17.77	0.21	17.64	0.18	17.67	0.23	17.86	0.34
FeO	8.19	0.32	7.65	0.24	7.70	0.21	7.62	0.19	7.73	0.34
MnO	0.21	0.06	0.19	0.04	0.19	0.03	0.18	0.04	0.16	0.07
MgO	2.10	0.22	2.13	0.22	1.95	0.15	2.00	0.10	2.18	0.17
CaO	5.15	0.42	5.03	0.40	4.74	0.32	4.80	0.19	5.15	0.22
Na_2O	4.45	0.39	4.72	0.24	4.56	0.29	4.58	0.59	4.71	0.23
K_2O	6.08	0.50	6.51	0.24	6.57	0.30	6.66	0.25	6.42	0.30
P_2O_5	0.73	0.06	0.80	0.05	0.79	0.04	0.79	0.05	0.76	0.07
Cl	0.29	0.04	0.24	0.03	0.25	0.02	0.23	0.04	0.21	0.02
Macro Unit	UPPER BROWN TUFF									
Locality	9 (Lipari)		5 (Vulcano)		4 (Vulcano)		5 (Vulcano)		5 (Vulcano)	
Unit	bt 13		bt 13		bt 14		bt 15		bt 16	
Sample	LIP07/19		VUL17/19		bt03/16 (V) 2 φ		bt04/16 (V) 2 φ		bt05/16 (V) 3 φ	
n	17		17		17		19		17	
	mean	1σ	mean	1σ	mean	1σ	mean	1σ	mean	1σ
(wt%)										
Total	97.90	1.00	99.17	1.03	97.82	0.79	98.31	0.61	98.00	1.06
SiO_2	60.80	1.95	59.12	0.65	56.96	1.03	58.16	0.87	58.06	1.38
TiO_2	0.64	0.04	0.65	0.05	0.68	0.05	0.68	0.03	0.68	0.04
Al_2O_3	16.37	0.41	17.30	0.36	17.12	0.26	17.14	0.17	17.47	0.41
FeO	5.72	0.61	5.94	0.56	6.88	0.53	6.32	0.38	6.28	0.28
MnO	0.11	0.02	0.12	0.04	0.16	0.05	0.15	0.05	0.15	0.04
MgO	1.85	0.52	1.78	0.11	2.20	0.29	1.86	0.29	1.94	0.27
CaO	3.89	0.97	3.87	0.19	4.73	0.53	3.99	0.59	4.25	0.58
Na_2O	4.09	0.43	4.38	0.14	4.24	0.19	4.39	0.25	4.27	0.45
K_2O	5.85	0.48	6.19	0.21	6.18	0.24	6.53	0.38	6.12	0.34
P_2O_5	0.43	0.06	0.47	0.07	0.61	0.04	0.57	0.04	0.54	0.05
Cl	0.23	0.02	0.18	0.05	0.24	0.04	0.21	0.02	0.25	0.01

Table 5

Average of major and minor element composition of secondary glass components inside Brown Tuffs units across the macro units included in the study. Totals are pre-normalised analytical totals. n = number of analyses used to calculate the average. Locality is referred to Fig.4. A complete geochemical dataset is provided in Supplementary material B.

Corresponding Pyroclastic Unit	Grey Porri Tuff		Grey Porri Tuff		Grey Porri Tuff		Perciato		Falcone	
Locality	8 (Lipari)		8 (Lipari)		1 (Lipari)		2 (Lipari)		4 (Lipari)	
Unit	bt 1/2		bt 3		bt 4		bt 8		bt 9	
Sample	LIP10/18 3φ		LIP07/18 3φ		bt09/16 (L) 3φ		bt12/16 (L)		LIP16/18 3φ	
n	3		2		3		15		4	
	mean	1σ	mean	1σ	mean	1σ	mean	1σ	mean	1σ
(wt%)										
Total	97.18	0.40	98.68	0.17	97.76	0.17	96.08	0.97	93.94	0.65
SiO_2	58.19	1.48	57.08	0.43	59.07	0.43	75.92	0.37	76.05	0.30
TiO_2	1.17	0.13	1.14	0.34	0.91	0.34	0.07	0.02	0.05	0.02
Al_2O_3	16.53	1.80	17.18	2.16	16.11	2.16	12.65	0.15	12.49	0.21
FeO	7.44	1.26	7.72	1.52	8.49	1.52	1.36	0.10	1.48	0.08
MnO	0.13	0.04	0.14	0.04	0.22	0.04	0.04	0.03	0.04	0.05
MgO	2.70	0.64	3.25	0.44	2.59	0.44	0.02	0.02	0.02	0.02
CaO	7.27	1.69	7.38	0.46	6.71	0.46	0.70	0.06	0.69	0.02
Na_2O	3.47	0.27	3.44	0.50	3.01	0.50	2.94	0.31	3.75	0.11
K_2O	2.47	0.85	2.02	0.35	2.30	0.35	5.99	0.27	5.10	0.14
P_2O_5	0.50	0.07	0.48	0.08	0.35	0.08	0.01	0.02	0.02	0.01
Cl	0.14	0.06	0.16	0.01	0.24	0.01	0.30	0.03	0.31	0.03
Corresponding Pyroclastic Unit	Monte Guardia		Monte Guardia		Monte Guardia		Vallone Del Gabellotto			
Locality	7 (Lipari)		12 (Lipari)		3 (Vulcano)		5 (Vulcano)			
Unit	bt 12		bt 12		bt 12		bt 16			
Sample	bt01/16(L)		LIP17/17		VUL09/17 -1φ		bt05/16 (V)			
n	17		8		3		3			
	mean	1σ	mean	1σ	mean	1σ	mean	1σ		
(wt%)										
Total	94.44	1.10	96.43	0.61	94.39	0.91	97.53	0.69		
SiO_2	76.10	0.27	76.42	0.42	75.55	0.16	75.37	0.42		
TiO_2	0.07	0.02	0.05	0.02	0.05	0.05	0.05	0.06		
Al_2O_3	12.51	0.07	12.28	0.29	12.59	0.08	12.72	0.32		
FeO	1.37	0.10	1.49	0.12	1.45	0.08	1.53	0.16		
MnO	0.08	0.04	0.05	0.02	0.05	0.04	0.05	0.01		
MgO	0.01	0.01	0.01	0.01	0.01	0.01	0.02	0.01		
CaO	0.69	0.04	0.67	0.05	0.72	0.04	0.71	0.04		
Na_2O	3.77	0.13	3.72	0.18	3.97	0.07	4.07	0.05		
K_2O	5.03	0.21	4.94	0.15	5.26	0.01	5.10	0.23		
P_2O_5	0.01	0.02	0.02	0.02	0.01	0.01	0.00	0.00		
Cl	0.35	0.04	0.35	0.03	0.34	0.02	0.38	0.02		

Table 6

Average of major and minor element glass composition of near-source Vulcano pyroclastic units included in the study.Totals are pre-normalised analytical totals. n = number of analyses used to calculate the average. Locality is referred to Fig.4. A complete geochemical dataset is provided in Supplementary material B.

Pyroclastic unit	Monte Molineddo 1		Monte Molineddo 1		Monte Molineddo 2		Monte Molineddo 3	
Locality	2 (Vulcano)		2 (Vulcano)		2 (Vulcano)		3 (Vulcano)	
Sample	VUL03/18 3φ		VUL04/18 2φ		VUL06/18 2φ		VUL04/17 1φ (component 1)	
n	23		6		10		10	
	mean	1σ	mean	1σ	mean	1σ	mean	1σ
(wt%)								
Total	96.29	0.81	98.54	1.05	98.58	1.23	97.96	1.60
SiO_2	57.43	0.33	56.73	1.16	53.08	1.35	53.33	0.31
TiO_2	0.98	0.05	0.99	0.08	0.86	0.07	0.76	0.04
Al_2O_3	16.09	0.33	16.28	0.69	17.06	0.56	17.56	0.24
FeO	7.96	0.19	8.15	0.82	9.09	0.70	8.28	0.33
MnO	0.17	0.03	0.19	0.03	0.17	0.04	0.22	0.04
MgO	1.85	0.14	1.97	0.28	2.66	0.22	2.43	0.11
CaO	4.61	0.14	5.14	0.61	6.39	0.38	5.38	0.80
Na_2O	4.12	0.12	4.05	0.18	4.25	0.30	4.56	0.32
K_2O	5.85	0.14	5.60	0.29	5.51	0.26	6.39	0.55
P_2O_5	0.76	0.03	0.69	0.05	0.69	0.04	0.73	0.06
Cl	0.19	0.02	0.22	0.08	0.26	0.04	0.36	0.08
Pyroclastic unit	Monte Molineddo 3		Punte Nere		Punte Nere		Punte Nere	
Locality			6 (Vulcano)		6 (Vulcano)		6 (Vulcano)	
Sample	BT03/20		VUL03/17 1φ		VUL02/17 1φ		VUL01/17 1φ	
n	42		13		14		9	
	mean	1σ	mean	1σ	mean	1σ	mean	1σ
(wt%)								
Total	97.79	0.30	97.06	1.17	97.19	1.39	98.54	1.18
SiO_2	53.51	0.28	56.87	0.55	56.09	0.44	60.32	1.72
TiO_2	0.73	0.04	0.68	0.04	0.67	0.04	0.60	0.06
Al_2O_3	17.18	0.14	18.18	0.23	18.03	0.17	16.76	0.35
FeO	8.24	0.24	6.14	0.17	6.38	0.50	5.73	0.58
MnO	0.16	0.02	0.16	0.05	0.15	0.04	0.10	0.07
MgO	3.05	0.15	1.66	0.09	1.82	0.18	1.71	0.37
CaO	6.63	0.23	3.74	0.21	4.07	0.32	3.59	0.66
Na_2O	3.91	0.13	4.37	0.59	4.46	0.43	4.23	0.20
K_2O	5.82	0.15	7.39	0.30	7.50	0.39	6.28	0.51
P_2O_5	0.52	0.05	0.52	0.03	0.54	0.02	0.50	0.11
Cl	0.24	0.02	0.29	0.04	0.28	0.02	0.19	0.06

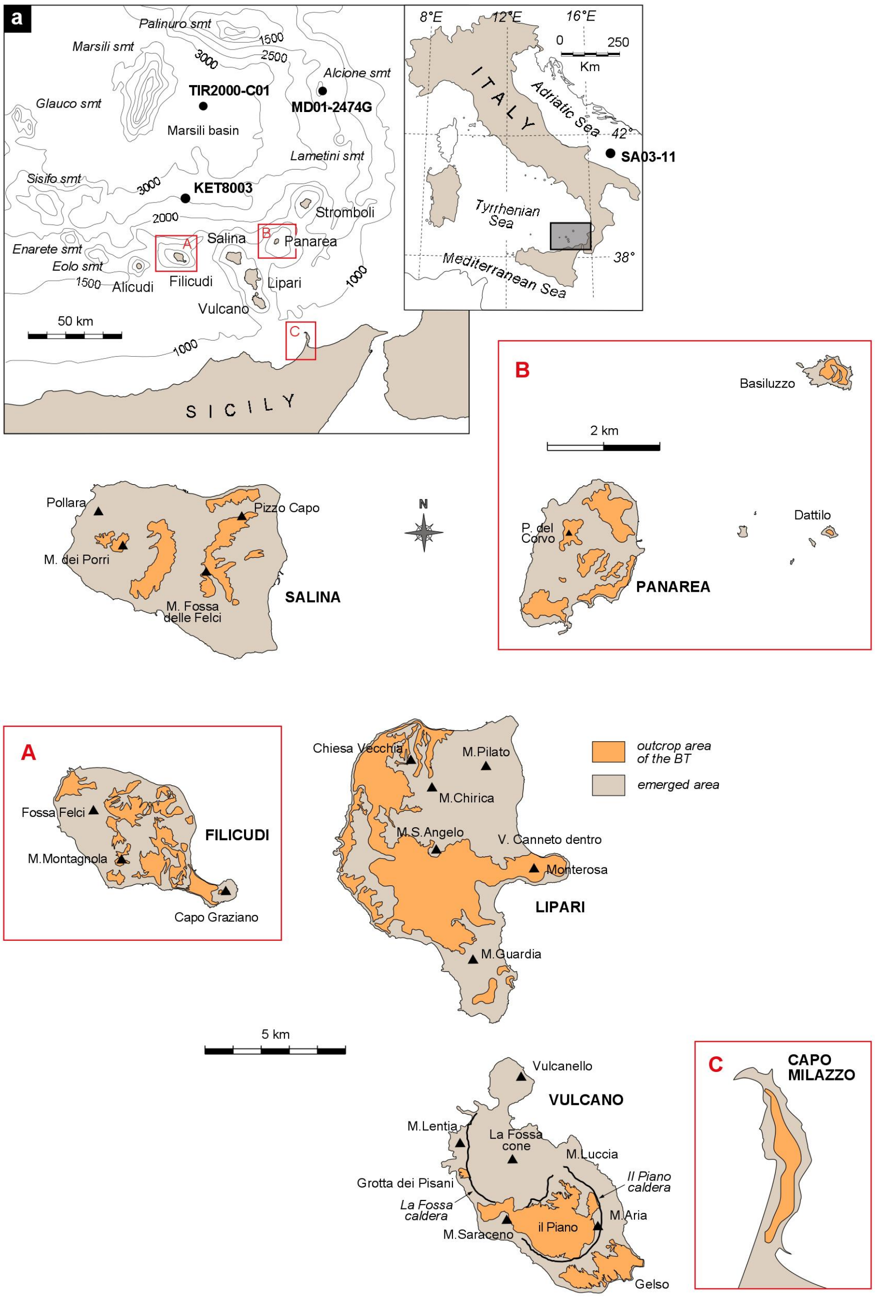

Fig. 1 - Meschiari et al.

Fig. 2 - Meschiari et al.

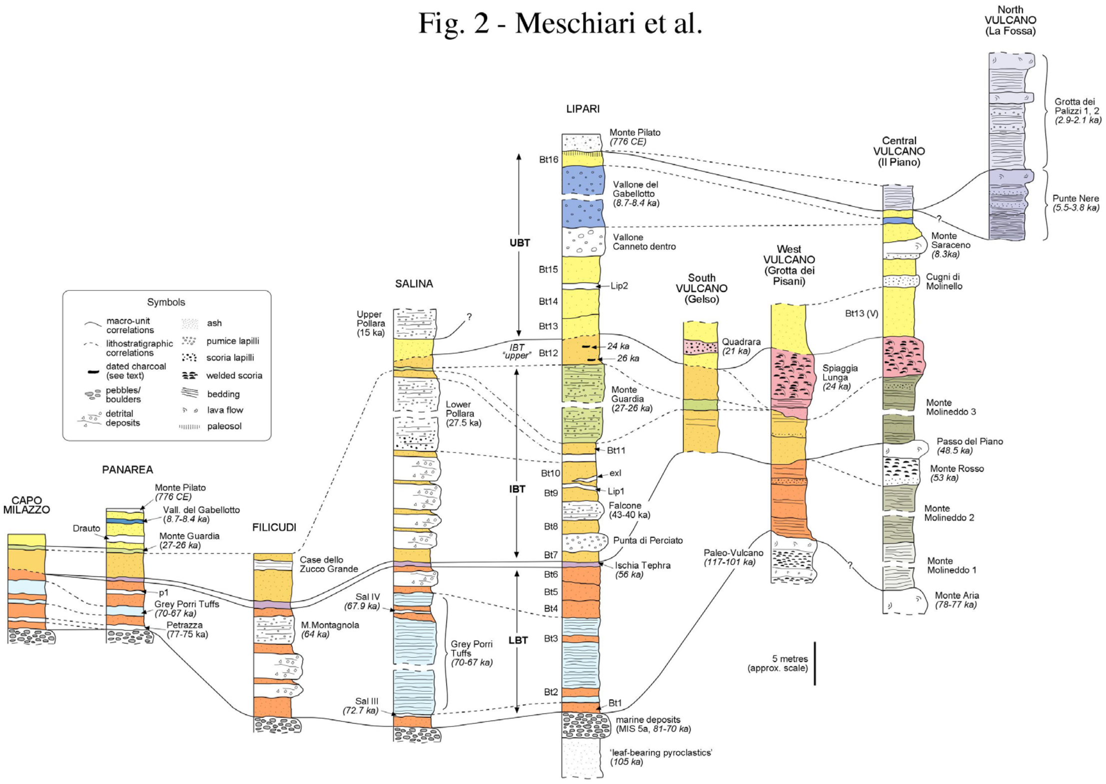

1360

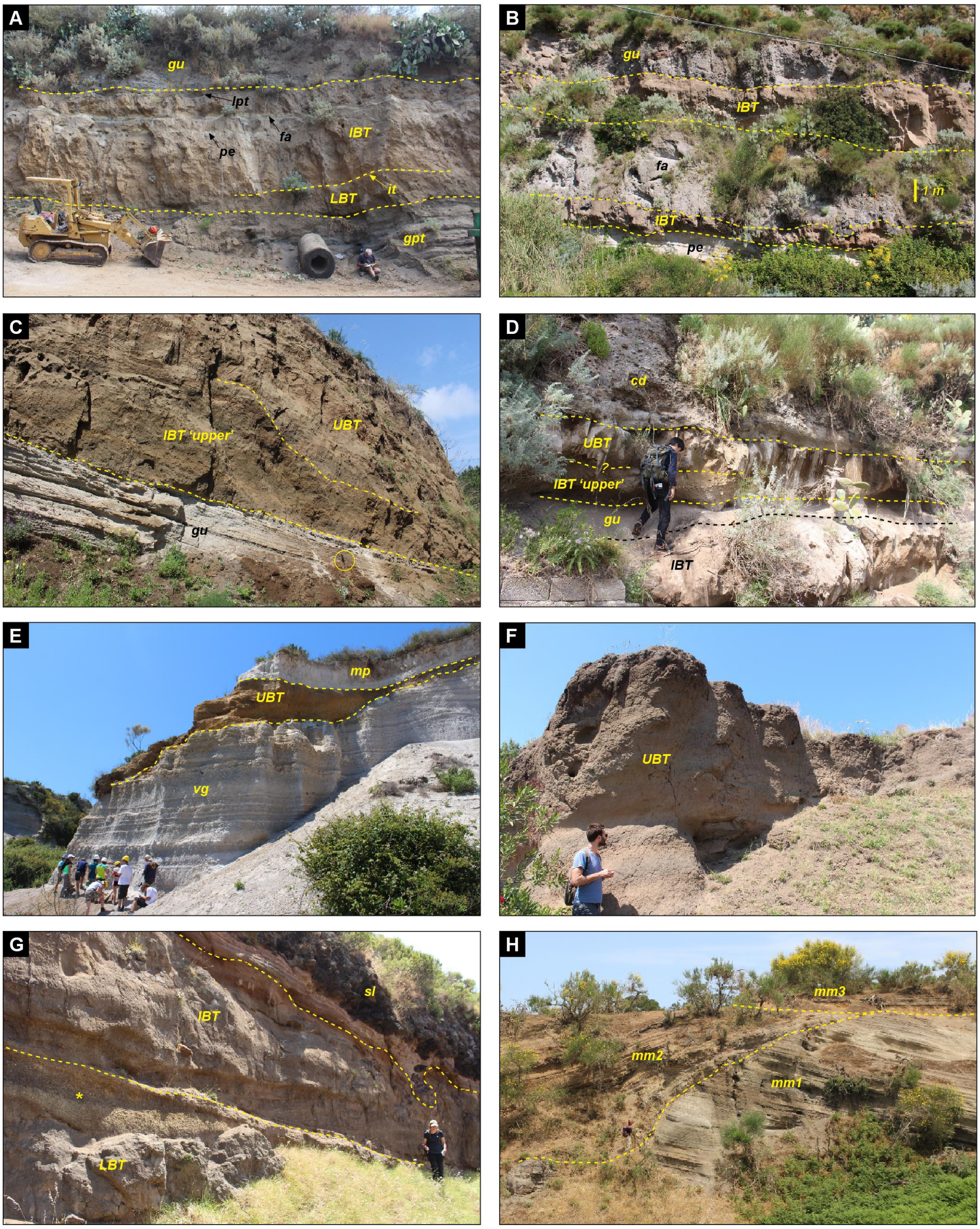

Fig. 3 - Meschiari et al.

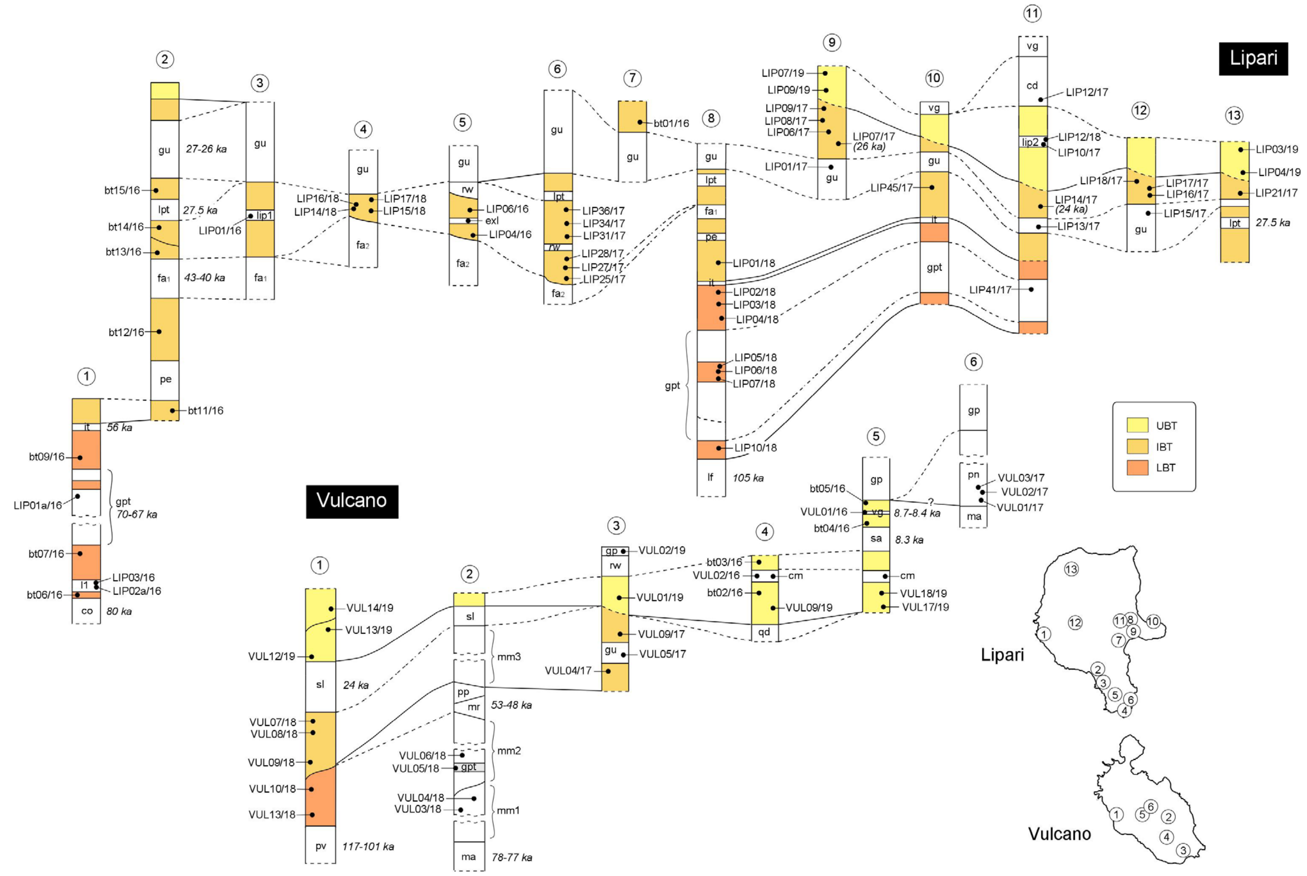

Fig. 4 - Meschiari et al.

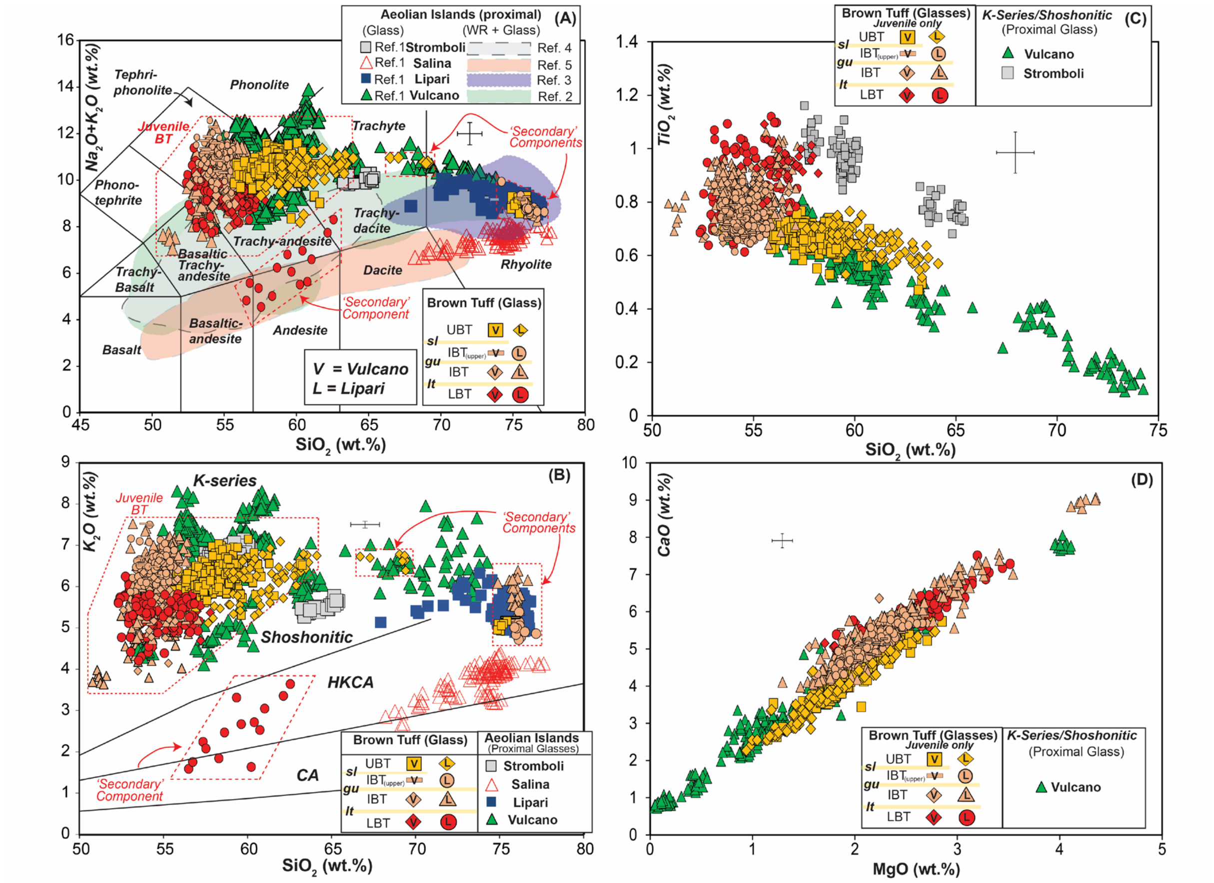

Fig. 5 - Meschiari et al.

Fig. 6 - Meschiari et al.

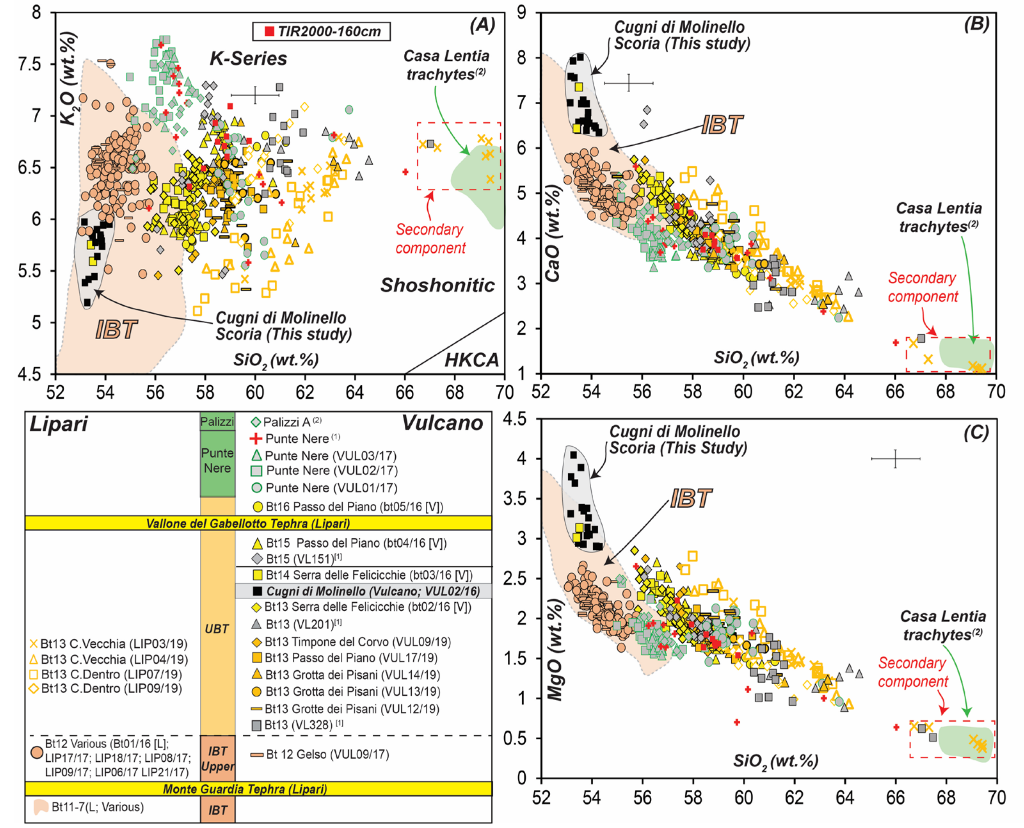

Fig. 7 - Meschiari et al.

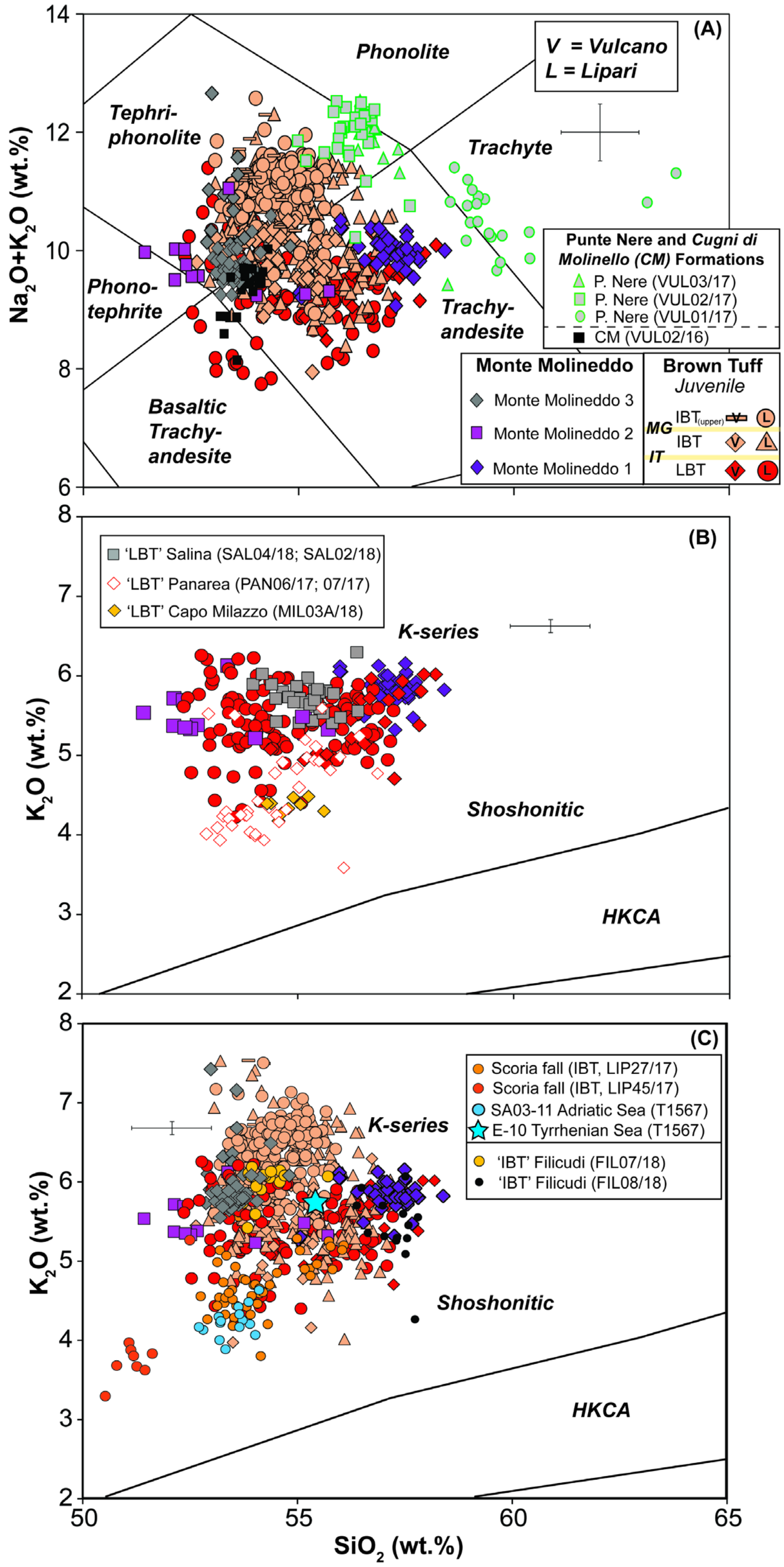

Fig. 8 - Meschiari et al.

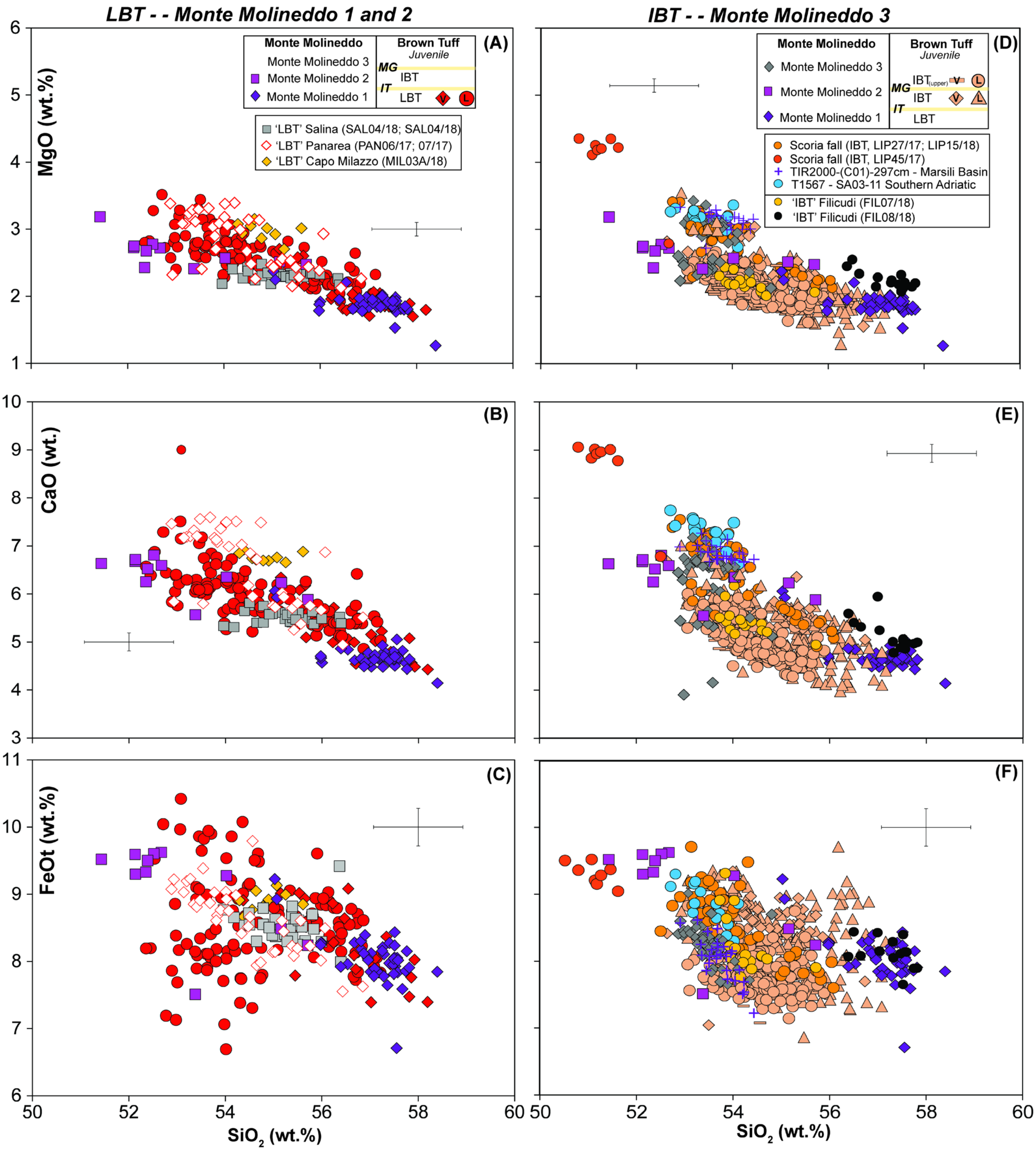

1368

Fig. 9 - Meschiari et al.

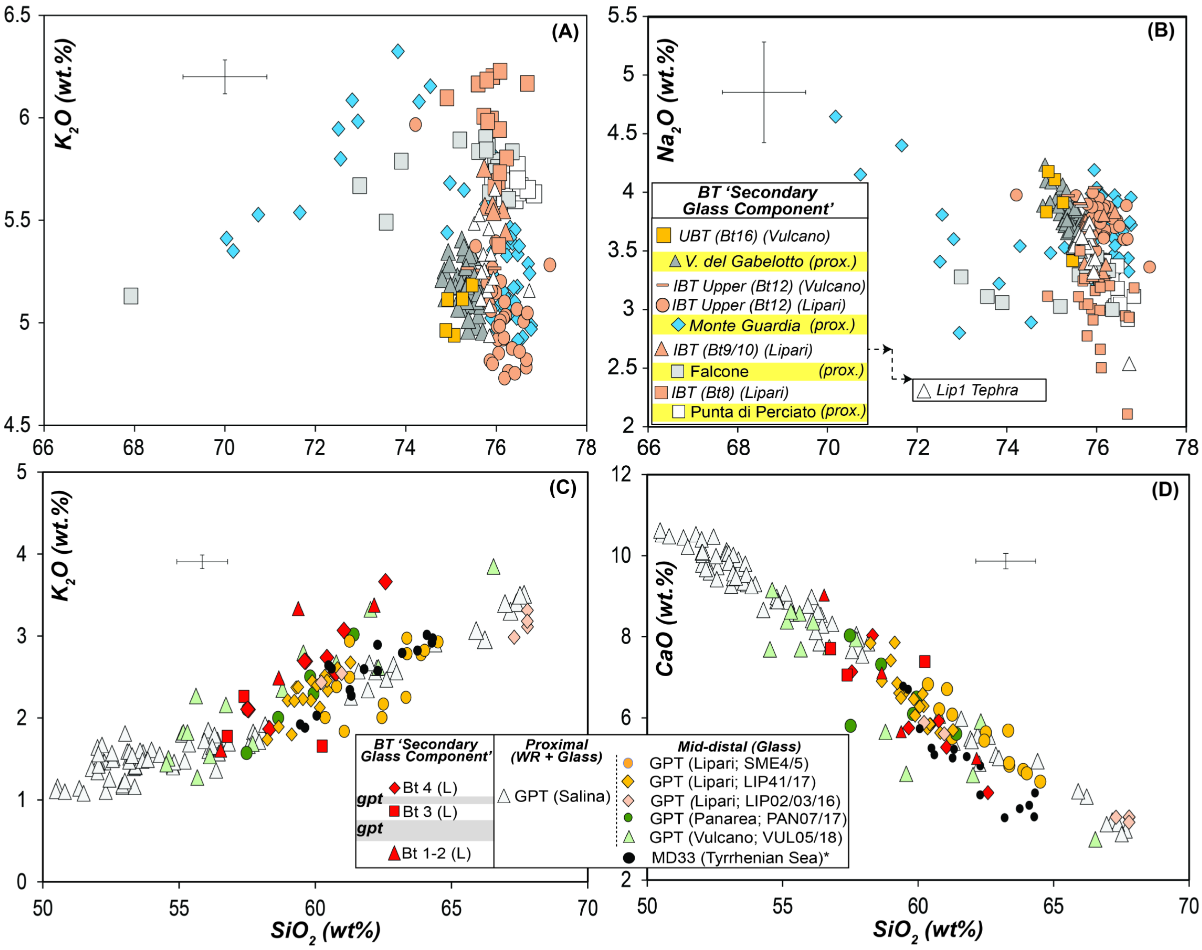

Fig. 10 - Meschiari et al.